

New zircon U-Pb ages for the lower Cantwell Formation: implications for the Late Cretaceous paleoecology and paleoenvironment of the lower Cantwell Formation near Sable Mountain, Denali National Park and Preserve, central Alaska Range, USA

Carla Susanne Tomsich¹, Paul J. McCarthy¹, Anthony R. Fiorillo², David B. Stone³, Jeff A. Benowitz⁴, and Paul B. O'Sullivan⁵

¹Department of Geology and Geophysics, and Geophysical Institute, University of Alaska, P.O. Box 755780, Fairbanks, Alaska 99775

²Perot Museum of Nature and Science, 2201 North Field Street, Dallas, Texas 75201

³Geophysical Institute, University of Alaska, P.O. Box 757320, Fairbanks, Alaska 99775

⁴Geophysical Institute, University of Alaska, P.O. Box 755940, Fairbanks, Alaska 99775

⁵Apatite to Zircon, Inc. 1075 Matson Road Viola, Idaho 83872-9709

ABSTRACT

The up to 4000 m-thick dinosaur (including birds) track-bearing Late Cretaceous (Campanian–Maastrichtian) lower Cantwell Formation, central Alaska Range, USA, was deposited at the suture zone between the North American continent and the allochthonous Wrangellia Composite Terrane during a time of protracted plate convergence. A combined total of 2500 m of measured section at Sable Mountain in Denali National Park and Preserve yields pterosaur manus tracks, non-avian and avian dinosaur footprints, diverse invertebrate traces, and abundant plant megafossils. Paleomagnetic data place the Cantwell basin between 65 to 75° N. The ecological data serve as climate proxies for high-latitude paleoenvironments. Two mid-section ash layers, separated temporally by 24 m of section, yield zircon U–Pb ages of 71.5 ± 0.9 Ma and 71.0 ± 1.1 Ma, respectively. These first radiometric ages for the lower Cantwell Formation suggest that exposures at Sable Mountain straddle the Campanian/Maastrichtian boundary, a time for which significant cooling and subsequent global sea level fall of an estimated 40 m is predicted. In this paper, we review sedimentological, paleoecological and paleomagnetic data and paleoclimate estimates previously reported from the Cantwell basin and interpret these data in light of the new age assignments. These new numerical ages enable more direct correlations between disparate fossil sites both within the Cantwell basin as well as across the Late

Cretaceous Arctic, with implications for floral and faunal exchanges between Asia and North America and ecological responses to paleoclimate changes.

Keywords: Late Cretaceous high-latitude dinosaur and fossil bird fauna, fossil flora, and paleoenvironments, U–Pb zircon geochronology, stratigraphic correlation, Prince Creek Formation, Chignik Formation, Cantwell Formation

INTRODUCTION

The biodiversity of ancient high-latitude ecosystems is not only of interest for the study of species evolution and palinspastic restorations, but also for the ecological response signal for an amplified climate change rate (Otto-Bliesner and Upchurch, 1997; Upchurch et al., 1998). Climate modelers thus focus increasingly on proxies of Arctic regions where taxonomic and physiological adaptations can be linked more clearly to climate perturbations. For pre-anthropogenic global climate models, temperature and precipitation proxies, which invariably are based on the geologic record, should be independent, temporally well-resolved, and representative of large geographic regions (Palaeosens Project Members, 2012). Given the limitations of available data for the distant past, the scale used by climate modelers is admittedly coarse (see, for instance, Markwick and Valdes, 2004), resulting in hypothesized long-term biological responses to climate change being incidental and blurring cause and effect relationships.

Radiometric dating allows a more direct correlation of paleoclimate records from different localities and different proxies and permits comparative evaluations of the factors contributing to regional climate variability such as vegetation distribution patterns, topography and paleogeography (Upchurch et al., 1998; Markwick and Valdes, 2004; Sewall et al., 2007; Spicer and Herman, 2010). Equally important, it provides valuable insights into regional dynamics of ancient terrestrial ecosystems, such as floral and faunal evolution and migration patterns.

The Late Cretaceous period was a time of significant climate instability. Continued, but cyclic polar warmth is predicted from the fossil biota and sedimentary rocks of Arctic and subarctic regions (e.g., Spicer, 1987; Herman and Spicer, 1995; Otto-Bliesner and Upchurch, 1997; Upchurch et al., 1998; Zakharov et al., 1999; Golovneva, 2000a; Spicer, 2003; Spicer and Parrish, 1990a,b; Rich et al., 2002; Fiorillo, 2006, 2008; Herman et al., 2009; Godefroit et al., 2009; Spicer and Herman, 2010).

A rich fossil floral and faunal record indicative of a temperate high-latitude paleoclimate is presently emerging from the Late Cretaceous sedimentary rocks of the Cantwell Formation in Denali National Park (formerly Mount McKinley National Park) and Preserve, Alaska, USA. The formation crops out on the northern flanks of the central Alaska Range (Fig. 1) and comprises a Late Campanian to Early Maastrichtian non-marine to marginal marine sedimentary succession (Ridgway et al., 1997), and an overlying Late Paleocene to Early Eocene volcanic succession (Gilbert et al., 1976; Csejtey et al., 1992; Cole et al., 1999), herein referred to as the lower and upper Cantwell Formation, respectively (Figs. 1 and 2).

The up to 4000 m-thick (Hickman, 1974; Hickman et al., 1990) non-avian and avian dinosaur track-bearing lower Cantwell Formation was deposited at the northern part of a Late Cretaceous suture zone between the Wrangellia Terrane, the northernmost subterrane of the allochthonous Wrangellia Composite Terrane, and the North

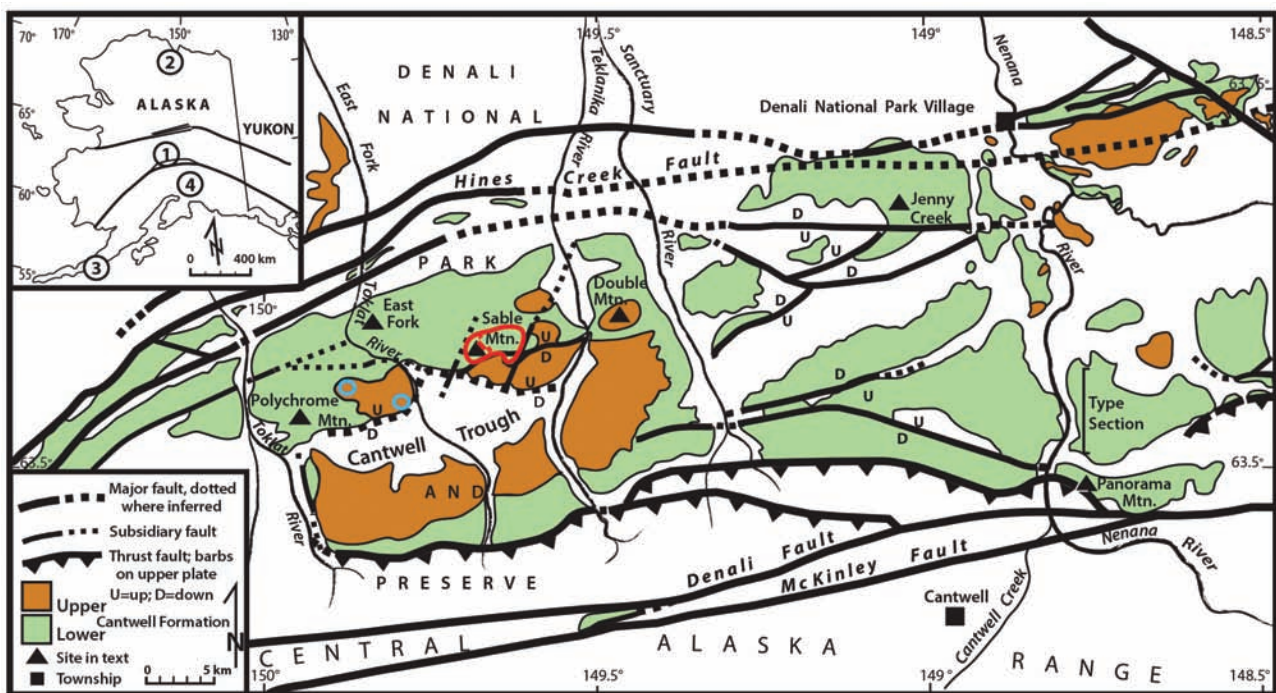


Fig. 1. Regional distribution of Cantwell Formation between longitudes -148.5 and -150.5° . Green fields: lower sedimentary unit; orange fields: upper volcanic unit; blank areas: all other lithologies and Quaternary alluvium. Red circle and lines: study area with composite measured section. Blue circles: paleomagnetic study sites of Sontag (1992). Geologic units from Csejtey et al. (1992), Gilbert and Redman (1975), and Wilson et al. (1998). Insert: Map of Alaska showing major strike-slip fault systems of central Alaska and locations of coeval Late Cretaceous fossil-bearing formations discussed in text: 1 = Cantwell, 2 = Prince Creek, 3 = Chignik, 4 = Matanuska.



Fig. 2. Cantwell Formation exposed at Sable Mountain. Reddish-weathered upper Cantwell volcanic strata in foreground are downfaulted against organic-rich sedimentary lower Cantwell Formation in the distance. A heterogeneous lithology is evident from numerous lateral and vertical facies changes. Shown exposure is ~1 km wide. View is to the northwest.

American continent during the final stages of accretion (Ridgway et al., 1997; Cole et al., 1999; Ridgway et al., 2002). Whereas previous research has focused on the tectono-sedimentary history of the Cantwell basin, current studies aim to reconstruct details of the paleoecology, paleoclimate and sedimentary subenvironments of this high-latitude basin for a fully integrated (geologic and paleoecological data) paleoenvironmental model. The discovery of a pterosaur and diverse dinosaur (including birds) ichnofauna at Sable Mountain, within Denali National Park, (Fiorillo et al., 2007, 2009a, 2011; Fiorillo and Adams, 2012; Fiorillo et al., 2014), in addition to a diverse invertebrate ichnofauna (Hasiotis et al., 2009, 2011) and plant fossils (Tomsich et al., 2010), suggests a remarkable paleo-Arctic biodiversity.

The presence of large-bodied herbivores in ancient polar regions is difficult to reconcile with extreme light and temperature seasonality. Yet,

dinosaur fossil localities are well-known from the Late Cretaceous circum-Arctic (see Parrish et al., 1987; Clemens and Nelms, 1993; Clemens, 1994; Rich et al., 1997, 2002; Fiorillo and Gangloff, 2001; Godefroit et al., 2009; Fiorillo et al., 2010). The biodiversity of the Cantwell Formation can be compared with the mid-to-late Maastrichtian Kakanaut Formation of the Okhotsk–Chukotka province in northeastern Russia (Golovneva, 1994; Golovneva, 2000a; Godefroit et al., 2009; Spicer and Herman, 2010) and with the polar dinosaur fossil-bearing section of the Late Cretaceous Prince Creek Formation on the North Slope of Alaska (Parrish et al., 1987; Parrish and Spicer, 1988; Spicer and Parrish, 1990a,b; Clemens and Nelms, 1993; Clemens, 1994; Rich et al., 2002; Fiorillo and Gangloff, 2000; Fiorillo, 2004, 2006; Gangloff and Fiorillo, 2010; Fiorillo et al., 2010; Fiorillo and Tykoski, 2012). However, identifiable bones in the Cantwell Formation have not been found to-date, and

the spatial and temporal relationships of complexly distributed fossil-bearing lithofacies at isolated, fault-bounded outcrops are still poorly understood.

In comparison, the Prince Creek Formation is well-exposed in a ~50 km long semi-continuous bluff along the Colville River. Strata include numerous bentonites and tuffs, and the ages of the fossil bone beds are fairly well-resolved (Conrad et al., 1992; Flaig, 2010; Flaig et al., 2013). Early Maastrichtian bone-bearing strata of the Prince Creek Formation are approximately the same age as sections of the lower Cantwell Formation. The Prince Creek vertebrate fauna thus hints at the kind of species that may have left footprints in the Cantwell Formation.

The age of the lower Cantwell Formation, on the other hand, is based on sparse pollen data collected from five widely spaced localities (Ridgway et al., 1997), and until now no reliable age constraint existed for the Sable Mountain area. Strata include few, mostly thin layers of highly altered bentonites that were preserved in local depressions. Recent advances in geochronological analyses of uranium and lead (U–Pb) isotope systems for residual uranium-rich minerals, such as zircon, provide new possibilities for obtaining high-resolution geochronological ages from sedimentary successions lacking datable fossils and unaltered potassium-bearing minerals required for K–Ar or $^{40}\text{Ar}/^{39}\text{Ar}$ dating. The laser ablation–inductively coupled plasma–mass spectrometry (LA–ICP–MS) technique is now widely applied, especially for large (≥ 100) zircon grain populations, as various statistical strategies have been adopted to account for isobaric interferences during analytical runs, determine detrital component, correct for common lead, and analyze zircon variability and error (Corfu, 2013). Here we report on the first radiometric ages obtained for two closely spaced lower Cantwell Formation bentonites from Sable Mountain and review regional paleoecological, paleoenvironmental and paleogeographical information to investigate the implications of improved correlations with coeval fossil-bearing sites of North America and northeastern Asia.

This research is part of an ongoing study in Denali National Park. Detailed measured sections (Fig. 3), facies analyses, channel trend mapping, and fossil and geochronological data are used to

characterize the sedimentary subenvironments, habitat conditions and paleoecological trends in order to determine influences on deposition and the paleoenvironment.

GEOLOGIC SETTING

Regional Geology

The geology of central and southern Alaska has been profoundly impacted by the juxtaposition of numerous terranes and continental slivers containing different rock types as old as the Proterozoic, and by geologic processes in effect during the past nearly 120 Ma including tectonic activity caused by the still-moving Pacific Plates. The Cantwell basin is an east–west-trending, ~135 km long and ~35 km wide structure bracketed by the Hines Creek Fault and the McKinley Fault strands at the northern apex of the arcuate Denali Fault (Fig. 1). The Denali Fault is a segmented 1200 km-long right-lateral transform fault system that bounds the large pericratonic Yukon Tanana Terrane of interior and eastern Alaska and British Columbia, Canada, and sheared-off continental margin slivers on the north side, and the Wrangellia Composite Terrane on the south side (Jones et al., 1983; Panuska and Stone, 1981; Stone, 1981; Nokleberg et al., 1985, 1994; Plafker and Berg, 1994; Ridgway et al., 2002; Nokleberg and Richter, 2007; Trop and Ridgway, 2007). The boundary represents the late Mesozoic suture zone or the Alaska Range suture zone (Ridgway et al., 2002). The Wrangellia Composite Terrane is southern Alaska’s largest accreted tectono-stratigraphic terrane assemblage and consists of the Wrangellia Terrane of central and south-central Alaska, the Peninsula Terrane of west-central and southwestern Alaska, and the Alexander Terrane of southeast Alaska (Nokleberg et al., 1994). The collision and accretion is thought to have been time-transgressive (Trop and Ridgway, 2007; Hampton et al., 2007) along the > 2000 km long boundary. In the northern part of this suture zone (which includes our study area), onset of accretion is constrained to the early Late Cretaceous (Nokleberg et al., 1994; Hampton et al., 2010). Between the Hines Creek Fault strand and the northern edge of the oceanic Wrangellia Terrane lies an accretionary and post-accretionary complex that includes juxtaposed slivers of dislodged stratigraphic assemblages of continental margin and

oceanic affinity, and syncollisional melange and thick siliciclastic deposits of an ocean basin that closed during the mid to early Late Cretaceous (Hampton et al., 2007; 2010). The turbiditic sediments that filled this basin are now widely exposed within a ~400 km long arcuate belt at the Alaska Range suture zone and are collectively assigned to the Kahiltna assemblage (Csejtey et al., 1992; Ridgway et al., 2002; Trop and Ridgway, 2007; Hampton et al., 2007; Hampton et al., 2010). Csejtey et al. (1992) postulate the thick flysch sequence to have been thrust-emplaced during the collisional orogeny. These accreted units are overlain by or are in fault-contact with post-collisional non-marine sedimentary and igneous rocks (e.g., Cantwell Formation and younger fluvial successions).

Following the accretion of the Wrangellia Composite Terrane, the southern margin of Alaska continued to grow by subduction, arc magmatism and accretion. Continued convergence in the Alaska Range suture zone resulted in folding, uplift and partial exhumation of post-collisional sequences in the Cenozoic (Trop and Ridgway, 2007; Benowitz et al., 2011, 2013). High heat flow, possibly due to oblique subduction of a mid-ocean ridge and a resultant mantle window, is the inferred cause of extensive early Tertiary intracontinental extension and plutonism (Bradley et al., 2003; Cole et al., 2006, 2007; Benowitz et al., 2012) that may have contributed to the deposition of the volcanic upper Cantwell Formation. Subsequent Cenozoic strike-slip faulting on the margin-parallel Tintina and Denali Fault systems, and associated strain partitioning of the intervening crust, led to widespread high-angle normal and reverse faulting and block rotation (Hickman et al., 1990; Csejtey et al., 1992; Plafker and Berg, 1994; Ridgway et al., 2002; Till et al., 2007a,b; Trop and Ridgway, 2007). Today, the Cantwell Formation is preserved in a regional synclinorium commonly referred to as the Cantwell Trough (Fig. 2).

The Cantwell Formation

The Late Cretaceous to early Tertiary Cantwell Formation comprises a lower non-marine to marginal marine sedimentary unit (Ridgway et al., 1997), and an upper, predominantly bimodal (mafic and felsic) volcanic unit (Figs. 1 and 2; Gilbert et

al., 1976; Csejtey et al., 1992; Ridgway et al., 1997; Cole et al., 1999). The lower Cantwell Formation is abundantly fossiliferous, and consists of numerous successions of conglomerate, sandstone, mudstone and, locally, thin coal seams and altered tuffs (Fig. 3). The sedimentary rocks rest unconformably on weakly metamorphosed and locally, intensely folded Late Jurassic to Cretaceous flysch deposits that may be correlative to the Kahiltna assemblage (see Csejtey et al., 1992; Ridgway et al., 2002); Triassic marine basalts; mid-Paleozoic to Triassic shelf-margin sedimentary strata of dismembered tectonostratigraphic terranes; and Proterozoic to early Paleozoic schists of the Yukon Tanana Terrane (Csejtey et al., 1992; Ridgway et al., 1997; Trop and Ridgway, 1997; Till et al., 2007).

The top of the lower Cantwell Formation is thought to have eroded to various depths (Wolfe and Wahrhaftig, 1970). A total thickness of up to 4000 m is estimated for the alluvial deposits near the basin axis from isopach mapping in the Nenana River corridor (Fig. 1) where the stratigraphy is best resolved (Hickman, 1974; Hickman et al., 1990). The fluvial succession is commonly intruded and overlain (locally on a shallow angular unconformity) by volcanic deposits of the upper Cantwell Formation. The igneous succession, preserved in local synclines and downfaulted blocks, comprises up to 2750 m of volcanic and subvolcanic flows, pyroclastic deposits, and associated volcanoclastic deposits (Cole et al., 1999). The igneous unit is often informally referred to as the Teklanika formation (Gilbert and Redman, 1975; Gilbert et al., 1976) or Teklanika volcanics (Sontag, 1992), but it has never been officially designated as a separate formation or member.

METHODS

Stratigraphic Analyses and Data Collection

Stratigraphic sections with a combined total of 2500 vertical m were measured and described in detail from 18 sites near Sable Mountain (Denali National Park, Alaska). A composite section for a 640 m long interval is depicted in Fig. 3, and the lithofacies are described in Table 1.

Paleocurrent trends were recorded from trough cross-beds. Trace fossils were photo-documented in the field and described in terms of location, rock type, and track size, shape, depth, and quality

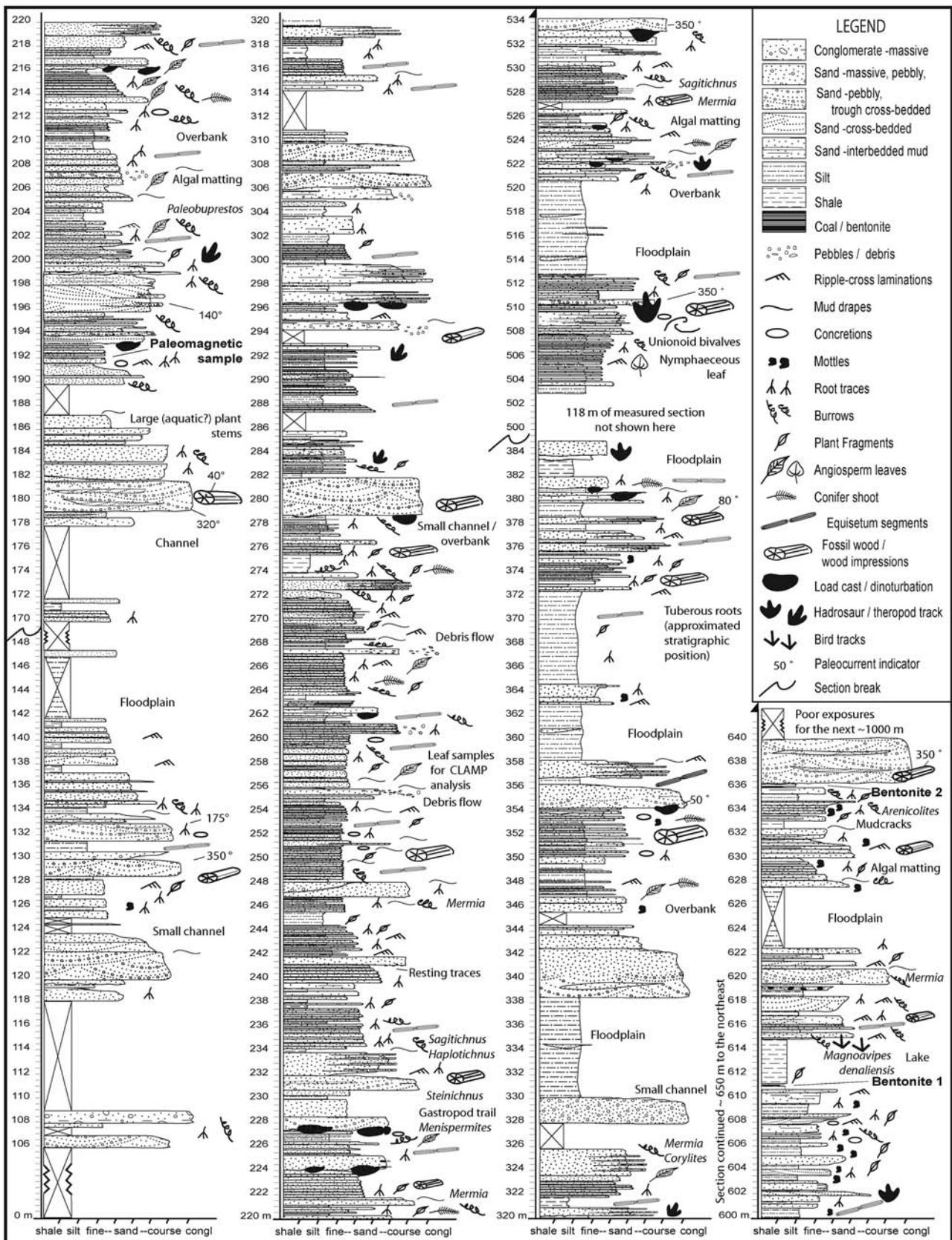


Fig. 3. Stratigraphic columns for a composite measured section at Sable Mountain, showing lithologies, sedimentary structures, fossils, and radiometrically dated bentonite horizons. See legend for explanations.

Table 1. Lithofacies and facies associations of the lower Cantwell Formation at Sable Mountain

Facies (Facies Association)	Thickness	Description	Interpretation
F 1 (FA 1) Matrix-rich, non-stratified, unsorted conglomerate	0.2 to 1.5 m average: ~ 1 m	Tabular or wedge-shaped, laterally discontinuous deposits locally encased in floodplain or channel facies. Contacts sharp or shallow irregular. Widths range from a few to 10's of meters. Texture massive with poorly sorted floating clasts up to 15 cm in diameter, woody debris and plant matter in muddy or sandy, organic-rich matrix. Capped by F 2, F 5, or F 7. Contains tree stump impressions and plant fossils.	Debris flow associated with bank or slope failure, storm events and high sediment supply (Harvey and Wells, 1987; Miall, 2006; Kumar et al., 2007)
F 2 (FA 1) Massive conglomerate	dm to 6 m average: < 2 m	Sharp-based tabular and shallow trough-shaped, laterally discontinuous deposits encased in floodplain or channel facies. Widths range from 10 m to 250 m. Texture matrix-supported and less commonly clast-supported. Poorly stratified subangular to well-rounded clasts are moderately sorted and weakly to locally well-imbricated. Average clast sizes range between 4 to 8 cm; maximum size is 15 cm. Polymictic clast lithology, including intraformational mud- and sandstones. Matrix fine to coarse-grained, predominantly subangular; well-cemented. Includes sandstone lenses and thin layers (up to 3 cm) of mudstone that divide deposits into multiple stories. F 2 commonly fines to stratified or massive medium-grained sandstone. Includes tree log or stump impressions.	Hyperconcentrated flow deposit as a result of high sediment supply and unconfined channel flow conditions on alluvial fan (Kumar et al., 2007). Textural variations suggest deposit is transitional to traction flow (Wells and Harvey, 1987; Miall, 2006).
F 3 (FA 2) Bedded conglomerate FA 2	dm to 2 m average: 1 m	Tabular and shallow lenticular-shaped clast and matrix-supported deposits co-occurring with F4, F5 and F6 to form bodies 10's of meters to up to 400 m wide. Clasts consist of moderately to well-sorted, subangular to well-rounded pebbles and cobbles that are planar bedded or trough cross-bedded. Clasts locally imbricated or aligned on low-angle foresets. Average clast diameter 3 to 5 cm, maximal 10 cm. Matrix medium to coarse-grained subangular sand that commonly fines to medium, horizontally stratified granular sand. Rare upward-coarsening. Single or multiple stories; include thin layers of mudstone and sandstone lenses. Mud drapes commonly on top. Tree log impressions common.	Traction flow deposits in gravelly braided channels on alluvial fan and in interfan areas including axial alluvial plain. Clasts interpreted as bedload and channel lag. Structures represent migration of channels and bars. Mudstone indicates rapid abandonment (Wells and Harvey, 1987; Kumar et al., 2007; Miall, 2006).
F 4 (FA 2) Pebbly sandstone	cm to 2 m average: 1.2 m	Tabular and shallow lenticular geometries. Pebbles angular to well-rounded, 0.3 to 5cm in size. Matrix coarse- to medium-grained. Beds horizontally or low-angle cross-stratified with pebbles on foresets. Normal and reverse grading; commonly grades into medium sandstone at top. Occurs in association with F 3, F 5, and F 6.	Traction flow deposits in sandy braided channel (Miall, 2006)
F 5 (FA 2) Cross-bedded coarse to fine-grained sandstone	0.3 to 1.5 m average: < 1 m	Planar cross-bedded bodies with granules or mud on foresets. Grains subangular to subrounded. Rare. Associated with sandstone facies F 4, F 6, F 7, and F 8.	Traction flow across a channel bar (Miall, 2006)
F 6 (FA 2) Coarse-to medium-grained sandstone	0.5 m to 8 m average: 0.9 m	Tabular and shallow lenticular geometries. Horizontally bedded or apparently massive with faint bedding structures. Forms sand lenses and multistory deposits. Grains subangular to subrounded and moderately sorted. Moderately cemented and rooted. Contains concretions and tree log impressions. Upper contacts predominantly sharp	Rapid deposition in confined and unconfined channels Amalgamated in confined channel. Massive sandstone may be homogenized by post-depositional burrowing or soft-sediment deformation

Table 1. Continued.

Facies (Facies Association)	Thickness	Description	Interpretation
F 7 (FA 2, FA 3) Massive medium-to fine-grained sandstone	0.2 to 4 m average: < 1 m	Tabular and shallow lenticular sandstone typically embedded in finer-grained deposits. Fining upwards fine-grained sandstone, not medium sandstone. Contacts commonly sharp. Well-indurated, but poorly cemented in a few places. Contains granules and small floating pebbles. Grains predominantly subangular and moderately-well sorted. Locally burrowed and rooted. May contain iron oxide nodules, <i>Equisetites</i> rhizomes and stems, lithified and partly coalified and sideritized wood, and impressions of tree trunks, stumps and roots, conifer shoot axes, plant tubers, and partial angiosperm leaves that were folded and/or fragmented during high energy transport.	Rapid deposition under waning flow stage in flood channel and unconfined overbank stream flow (Bull, 1977; Miall, 2006). Presence of burrows and roots suggests periodic fluctuations of water table.
F 8 (FA 2, FA 3, FA 4) Tabular trough cross-bedded coarse to fine-grained sandstone	0.3 to 1.5 m average: < 1 m	Occurs in form of extensive sheets and shallow lenticular bodies. Deposits typically are sharp-based and upward fining. Grains are subrounded to rounded; include granules and minor small pebbles. Amplitude of trough cross-beds 2 to 15 cm. Burrowed and moderately rooted. May contain <i>Equisetites</i> rhizomes and stems, lithified wood, conifer shoots, and angiosperm leaf impressions. Associated with F 5, F 6, F 7, F 9, and F 10.	High-density flow or unconfined flow (including sheet-flood/ stream flow; Bull, 1977; Miall, 2006) deposits in distal alluvial fan and proximal alluvial plain settings. F 8 also occurs in inferred channel bar and crevasse splay deposits
F 9 (FA 4) Ripple-cross-laminated to massive fine- to very fine-grained sandstone	<5 cm to 1.5 m average: < 1 m	Tabular or lenticular bodies. Occurs in association with F 7, F 8, F 9, and F 11. Contacts can be gradational or sharp. Grains subangular to subrounded. Ripples include climbing ripples and herring bone patterns. Burrowed and moderately rooted. Contains conifer sprigs, leaves and cones, <i>Equisetites</i> rhizomes and stems, wood and angiosperm leaf impressions at base.	Overbank including crevasse splay channel deposits. Ripples indicate unidirectional flow. Climbing ripples suggest rapid sedimentation and herring bone structures signify reverse flow direction (Miall, 2006). Burrows and roots signal a fluctuating water table.
F 10 (FA 5) Interbedded fine to very fine-grained sand- and mudstone	<5 cm to > 10 m average: < 1 m	Numerous vertical successions of laterally continuous centimeter- to decimeter-scale interbeds form stacks 10's of meters thick. Sandstone is massive or rippled. Contains concretions, iron nodules, roots, abundant plant megafossils, and beetle and freshwater crustacean feeding traces.	Overbank deposits under waxing and waning flow stages on levee or distal crevasse splay. Well-preserved plant fossils indicate rapid deposition and short transport distance.
F 11 (FA 5) Siltstone	cm to >10 m average: 10 cm	Dark grey to black organic-rich siltstone. Commonly interlaminated with very fine sandstone and mudstone. Contains conifer needles, <i>Equisetites</i> rhizomes, carbonaceous roots and other plant fragments, iron concretions or nodules. Relief at top common.	Vegetated floodplain, lake, and pond settings. Abundant organic matter, nodules and concretions suggest high water table on alluvial fan and proximity to alluvial channels.
F 12 (FA 5) Organic-rich mudstone	mm to 1 m	Dark grey clay-rich siltstone and shale. Locally calcareous and yellow-weathering. Forms mud drapes and lenses. Mudcracks or irregular relief at top. Commonly contains plant fragments and trace fossils such as algal matting, <i>Mermia</i> and <i>Cochlichnus</i> .	Suspension settling from stagnant flood waters in floodplain lows; abandoned channel fill; bar tops (Miall, 2006).
F 13 (FA 6) Carbonaceous shale	cm to 10 m average: 20 cm	Dark grey to black; organic-rich. Locally calcareous. Mudcracks or irregular relief at top. Commonly seen in form of black or yellow-weathering rip-up clasts. Contains <i>Equisetites</i> segments, small, frequently coalified, plant fragments, rootlets, iron oxide nodules, and freshwater bivalve and gastropod shells and trails.	Backwater swamps and marshes proximal to streams (Miall, 2006)

Table 1. Continued.

Facies (Facies Association)	Thickness	Description	Interpretation
F 14 (FA 6) Coal	0.5 to 2 cm	Rare thin coal seams up to 2 cm thick. Laterally discontinuous. Commonly associated with bentonite.	Decaying plant matter in backwater swamps and marshes.
F 15 (FA 6) Bentonite	0.5 to 4 cm average: 1 cm	Volcanic ash deposit altered to white or light brown clay. Rare and discontinuous over 20 m. Commonly associated with thin coal seams. Contains minor amounts of zircon, apatite, volcanic glass, quartz, and altered feldspar.	Suspension settling in backwater ponds and lakes
F 16 (FA 1) Organic-rich gritty mudstone	0.5 to 1.5 m average: ~ 1 m	Laterally discontinuous, commonly wedge-shaped, unsorted, non-stratified deposits with variably sized free-floating small clasts, woody debris, plant fragments, mud rip-up clasts and sand and granule-sized grains in organic-rich mudstone matrix. Poorly consolidated. Sharp undulated bases and tops. Incorporates in-situ tree stump impressions and small unionid bivalves and gastropods that are commonly attached to plant stems.	Gravity mud flow deposit associated with slope or bank failure on alluvial fan, and along channel and lake margins (Bull, 1977; Miall, 2006).
Facies 17 Igneous rocks		Mafic dikes, sills and plugs consisting of aphanitic basalt to rare microcrystalline gabbro metamorphosed to greenschist facies. Host sedimentary rocks are locally hornfelsed.	Subterranean lava flows and intrusions of Latest Cretaceous and early Tertiary age.

of preservation. All trace fossils were analyzed for potential track-maker identification, animal size, social behavior, diversity and depositional environment. Fossil plant information was compiled on taxonomy, distribution, and community and lithofacies associations from on site outcrops and samples collected from float. We note here that in compliance with National Park regulations and permit application agreements, quarrying was not conducted. Palynomorphs were extracted from siltstones and shales and analyzed under the microscope for taxonomic identification and species distribution where possible. Collected plant megafossils and palynological slides will be archived at the University of Alaska Museum of the North.

Geochronological Analyses

Bentonite samples were collected from two volcanic ash layers at Sable Mountain, spaced 24 m apart in vertical section (Fig. 3). Bentonite 1 is a ~2 cm thick, brown-weathering altered tuff that consists of clay with minor zircon, apatite, altered feldspars,

and volcanic glass. Bentonite 2 is a ~10 cm thick, white-weathering tuff with a similar mineralogy. Both bentonites are bracketed by thin coal seams and are laterally discontinuous. The samples were brought to the University of Alaska Geochronology Laboratory where they were washed repeatedly to remove all clay, allowing time for the heavier minerals to settle between rinses. The mineral separates were sent to Apatite to Zircon, Inc., Viola, Idaho, USA, where zircon grains were isolated, mounted in epoxy, and polished for a LA-ICP-MS (laser ablation-inductively coupled plasma-mass spectrometry) analysis. The ablation was conducted at the Donelick Properties dba Institute on a Resonetics Resolution M-50 instrument using an ArF Excimer 193 nm laser and a spot diameter of 26 μm. Inductively coupled plasma mass spectrometry measurements were made on an Agilent 7700X Quadrupole ICP-MS. To calibrate fractionation factors for the relevant isotope ratios and determine absolute errors, two zircon U-Pb age standards with conventionally accepted ages of 1099.00 Ma (primary standard)

and 1065.40 Ma (secondary standard) were scanned prior to, during, and after each standard and sample batch spot analysis. Results were smoothed to establish collective values for each sample analysis session; these were then used to correct for cumulative radiation damage (for more detailed information on calibration procedures, see Donelick et al., 2010). Concordance was monitored separately for each ablation spot. Ages for the ratios $^{207}\text{Pb}/^{235}\text{U}$, $^{206}\text{Pb}/^{238}\text{U}$, and $^{207}\text{Pb}/^{206}\text{Pb}$ were calculated for each scan (25 to 32 individual scans performed on each spot) and checked for concordance; concordance here was defined as congruence of all three isotopic ages at the 2σ level. If the number of concordant data scans for a spot was greater than zero, the more precise age from the concordant-scan-weighted ratio $^{207}\text{Pb}/^{235}\text{U}$, $^{206}\text{Pb}/^{238}\text{U}$ or $^{207}\text{Pb}/^{206}\text{Pb}$ was chosen as the preferred age. $^{206}\text{Pb}/^{238}\text{U}$ ratios were used to calibrate ages for grains younger than 1.1 Ga, and $^{207}\text{Pb}/^{235}\text{U}$ ratios were used to calculate ages for grains older than 1.1 Ga. Asymmetrical negative and positive errors for each age were calculated by subtracting and adding, respectively, the isotopic ratio errors in the appropriate age equation (Chew and Donelick, 2012). Both samples were scanned and re-scanned in 2 separate sessions. Twenty-five single grain analyses per sample is standard practice for the constraint of

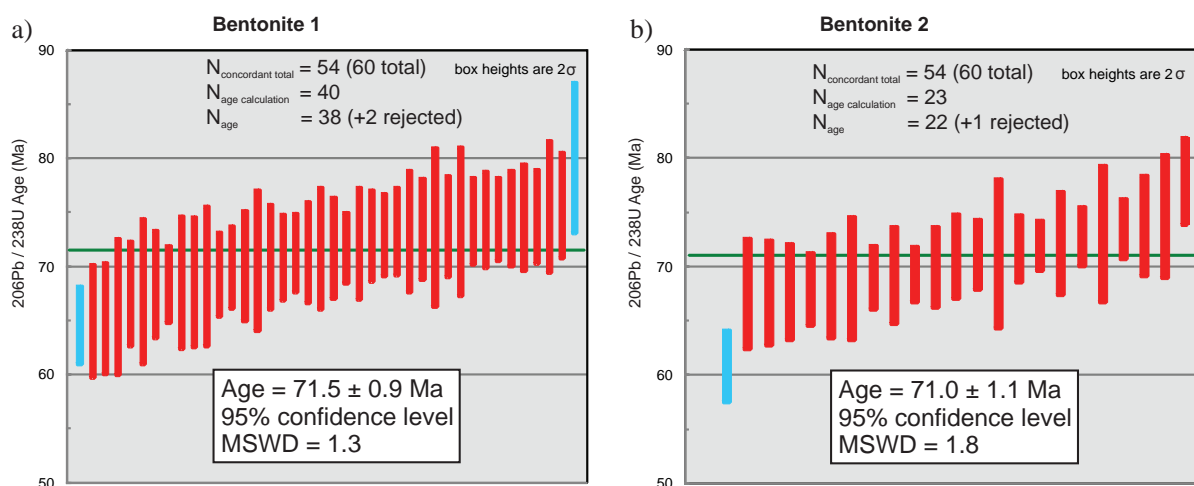
the crystallization age of a tephra. Additional single grain spot analyses were performed to identify potential detrital and xenocrystic components. The results for the measured isotope ratios and preferred ages are listed in Appendix A, Tables A-1 and A-2.

The preferred ages were filtered according to the probable age, e.g., grains older than 81 Ma were considered detrital, and grains younger than 60 Ma were also excluded on grounds of improbability. The latter may reflect localized anomalous concentration of uranium within a grain or Pb loss. In addition, error size was limited to 10% at the 2σ level. The remaining probable ages were used to calibrate the weighted mean age for each sample using Isoplot (Ludwig, 2003). The data were plotted as histograms showing concordant and overlapping results for single zircon grain analyses and the weighted mean age for each sample (Figs. 4a and 4b).

PREVIOUS WORK

Lithofacies and Depositional Models

The lower Cantwell Formation was first described by United States Geological Survey (U.S.G.S.) geologist G. H. Eldridge (1900) from the east bank of the Nenana River near Panorama Mountain ~22 km south of Denali National Park during a reconnaissance study in 1898. The site



Figs. 4 a), b). Histograms showing concordant results and overlap for LA-MS-ICP single zircon grain analyses. Weighted mean U-Pb ages are given by the green bar. 4a) Bentonite 1. The weighted mean age is 71.5 ± 0.9 Ma based on 38 single grain ages. 4b) Bentonite 2. The weighted mean age is 71.0 ± 1.1 Ma based on 22 single grain ages. Two grains from Bentonite 1 and 1 grain from Bentonite 2 (blue bars) were rejected because they do not overlap the weighted average and error margin of the accepted single zircon grain ages (at a modified 2-sigma error). Data is plotted in Isoplot (Ludwig et al., 2003).

later became the type section locality for the sedimentary succession (Capps, 1940; Wolfe and Wahrhaftig, 1970). Initial geologic investigations into the Cantwell Formation were aimed at resource estimation and resolving the geologic history of the Alaska Range. With the advance of plate tectonics and large-scale fault displacement concepts in the latter half of the nineteenth century, interest shifted to intracontinental basin evolution and the accretionary history of oceanic terranes.

The sedimentary succession has been described from a number of places and the complexity of lithofacies distribution was emphasized by all authors (Pogue, 1915, Capps, 1919, 1940; Wolfe and Wahrhaftig, 1970; Hickman, 1974; Billingsley, 1977; Stanley, 1987; Hickman et al., 1990; and Csejtey et al., 1992). Capps (1919, 1940) described lithologies and structures from a number of sites in Denali National Park and remarked on the heterogeneity of the rocks and their relationship to adjacent lithological units. Hickman (1974) isopach-mapped the distribution of the lower Cantwell Formation in the eastern parts of the Cantwell basin along the Nenana River corridor (Fig. 1) and outlined an east–west-trending southward deepening basin and several subbasins that are oriented obliquely to the basin margins.

Believing the sedimentary and volcanic members both to be of early Paleocene age, Hickman et al. (1990) characterized the Cantwell basin as a pull-apart structure that had formed in response to early Tertiary strike-slip deformation along the Denali Fault. Csejtey et al. (1992) contended that the siliciclastic sedimentary fill records regional crustal shortening associated with the amalgamation of the Wrangellia Composite Terrane. From a structural analysis, Cole et al. (1999) established multiple episodes of syn- and post-depositional deformation caused by initial northward thrusting followed by post-volcanism northwest-ward thrusting and subsequent strike-slip faulting along the Denali Fault system. The most comprehensive study of the lower Cantwell Formation thus far was conducted by Ridgway et al. (1997) and Trop and Ridgway (1997) who used paleoflow directions, grain size and facies trends from eleven sites across the basin to interpret the depositional environment as a stream-dominated alluvial fan system drained by an eastward-flowing

sandy-braided axial river. Based on their revision of the age of the sedimentary succession (Campanian / Early Maastrichtian), basin-wide facies distributions, and evidence for intraformational unconformities and growth strata, Ridgway et al. (1997) re-interpreted the Cantwell basin as a syn-orogenic thrust top basin that formed in the later stages of plate convergence between the Wrangellia Terrane and the late Mesozoic continental margin of North America. In this model, the Hines Creek Fault (Fig. 1) is an active thrust fault that underlies the leading thrust panel of a northward-propagating fold-and-thrust sheet on which the Cantwell basin formed.

From their regional facies analysis of the lower Cantwell Formation, Ridgway et al. (1997) defined five facies associations as follows:

- i) cobble conglomerate, thin mudstone and coal seams—interpreted as proximal braided stream
- ii) pebble conglomerate, sandstone and mudstone—interpreted as braided stream
- iii) interbedded sandstone and mudstone—interpreted as sheetflood
- iv) conglomerate and cross-bedded sandstone—interpreted as axial sandy river
- v) sandstone and mudstone—interpreted as lacustrine and lacustrine deltaic deposits.

According to these authors, the coarsest-grained facies are located near the northern basin margin and facies fine toward the basin axis. The lithology is polymictic, and clast composition varies greatly between outcrops reflecting a variety of different sediment source areas. On the basis of the facies distributions, Ridgway et al. (1997) interpreted the deposition as a stream-dominated alluvial fan system in a two-sided asymmetrically aligned basin drained by an axial sandy braided river.

The Age of the Lower Cantwell Formation

For nearly a century, age estimates for the non-marine to marginal marine (Ridgway et al., 1997) lower Cantwell Formation were based on diverse, but often poorly preserved fossil florules that included fragmentary angiosperm leaf impressions that reflected a broad stratigraphic range and morphological variation. The first age assessments were based on sparse material collected from single sites rather than from a combined data set, and results thus ranged from early Cretaceous

to Eocene (Pogue, 1915; Capps, 1919; Imlay and Reeside, 1954; Wolfe and Wahrhaftig, 1970). In 1937, Paleobotanist Ralph Chaney made generic and species identifications for 8 specimens from a larger collection of fragmentary plant fossils from the northern part of the basin and cautiously assigned a Cretaceous age to the formation (Capps, 1940). In a reevaluation of Chaney's taxonomic assignments, Wolfe (in Wolfe and Wahrhaftig, 1970) identified four taxa also known from the Paleocene Chickaloon Formation of southern Alaska and consequently assigned a Paleocene age to the formation. This early Tertiary age designation remained accepted even as subsequently published whole-rock and single mineral K–Ar ages for igneous intrusions indicated a much older age for the sedimentary sequence (Hickman, 1974; Hickman and Craddock, 1976; Sherwood and Craddock, 1979). Recalculated K–Ar ages for these intrusions range from 79.1 ± 6.0 to 71.9 ± 2.6 Ma (Csejtey et al., 1992).

More recently, less ambiguous age constraints brought clarity on several levels. From sparse fossil pollen data obtained for a basin-wide tectonostratigraphic study, Ridgway et al. (1997) were able to assign a Late Campanian and early Maastrichtian (~80 to ~70 Ma) age to a number of outcrop exposures of lower Cantwell Formation. Using newer $^{40}\text{Ar}/^{39}\text{Ar}$ techniques, Cole et al. (1999) subsequently re-dated the volcanic upper Cantwell Formation to 60 to 55 ± 0.2 Ma, revealing thereby a 10 to 15 Ma hiatus during which upper layers of the lower Cantwell Formation were eroded.

The Late Cretaceous age for the terrestrial sedimentary sequence then became a driving factor in the search for paleoecological data. The new age designation proved to be in good agreement with first dinosaur footprint documentations in the Cantwell Formation near Sable Mountain and Double Mountain in 2005 (Fiorillo et al., 2007). Since then, the paleoecological database has grown considerably enumerating thousands of dinosaur tracks while adding bird and pterosaur tracks to the list. From their palynological analyses, Ridgway et al. (1997) determined that some sections (Double Mountain and Jenny Creek) are entirely of Campanian age, while others (Polychrome Mountain, East Fork Toklat River and Dean Creek) include the early Maastrichtian.

Several palynological samples we processed for chronostratigraphic control proved to be inconclusive. Fossil pollen in the lower Cantwell Formation is commonly poorly preserved, and yields were inadequate to confidently assign an age to any outcrop. It appears that palynomorphs were degraded by heat, either due to Tertiary volcanism or burial, or both.

Paleolatitude of the Lower Cantwell Formation

Paleomagnetic pole positions and the composite apparent pole wander path (APW) for North America suggest that the northern geographic pole was positioned close to the coast of northwestern Alaska starting at about 130 Ma (Kent and Irving, 2010). Between ~120 and ~50 Ma, the North Pole remained at a relative standstill less than 1000 km off the northern Alaskan and northeastern Russian coastlines (present-day geography). This coincides with a time during which several floral turnovers took place. Most notably is the replacement of coniferous-dominated biota with northward migrating angiosperm communities leading to development of the mixed polar broad-leaved deciduous forest (Wolfe, 1987; Spicer et al., 1987; Spicer, 2003). Paleolatitude estimates for the Paleocene Cantwell basin range from $83^\circ \text{N} \pm 9^\circ$ (Hillhouse and Grommé, 1982), to $75^\circ \text{N} \pm 6^\circ$ (Sontag, 1992), to $71^\circ \text{N} \pm 10^\circ$ (Hillhouse and Coe, 1994). All of these calculations are based on paleomagnetic poles determined from the volcanic upper Cantwell Formation.

Previous paleomagnetic results for the lower sedimentary strata were found to be inconsistent and were not further evaluated. To test this further, we analyzed the magnetic properties of a single, spatially oriented organic-rich siltstone/very fine sandstone sample with preserved bedding structures and very few roots indicating only insignificant post-depositional sediment modification. The sample was collected from our composite section at a stratigraphic height of 191 m (Fig. 3).

Tilt-corrected magnetic inclination and declination for this sample were measured in the Paleomagnetism Laboratory of the University of Western Washington and yielded -65.4° and 149.7° , respectively. The demagnetization steps reveal that magnetic remanence is preserved. The measured magnetic inclination gave a paleolatitude of 47.5°

N. This number represents an anomalously low paleolatitude. One source for bias is an inclination error in sedimentary rocks caused by the shallowing of the magnetic inclination as a result of burial compaction and/or initial depositional factors. Such shallowing is common in clay-rich terrestrial sedimentary rocks; however, when a correction factor for the predicted mean flattening under compaction of 0.55 is applied (see for instance Kent and Irving, 2010), the paleolatitude increases to a more plausible 63.3° N. The result, which we recognize has no statistical value, is displayed in Table 2 to show that there is potential for future magnetostratigraphic and paleomagnetic studies to be successful. For comparison, we also reprint in Table 2 the results from a paleomagnetic study conducted by Sontag (1992) on upper Cantwell Formation volcanic rocks from the East Fork Toklat River and Polychrome Mountain located about 7 and 10 km, respectively, to the west of our study site.

RESULTS

Stratigraphic Analyses

The sedimentary facies documented along the incised ridges of the 1805 m tall Sable Mountain are described in Table 1 and are graphically depicted in Fig. 3. Therefore, we provide only a brief description of the lithofacies here.

The coarsest-grained deposits consist of tabular and shallow lenticular-shaped, laterally discontinuous bodies of predominantly matrix-supported and moderately sorted pebble to cobble conglomerate up to 6 m thick. Subangular to well-rounded polymictic clasts have a wide range of sizes between < 1 and 15 cm in diameter. The texture is massive to trough cross-bedded and includes sandstone lenses. Conglomerates typically fine upward to a medium-grained granular sandstone that is capped by mud drapes.

The sandy fraction consists of tabular to shallow lenticular trough cross-bedded sandstone and pebble sandstone up to 2.5 m thick; horizontally bedded (rarely cross-stratified) to massive upward-fining coarse to medium-grained sandstone up to a rare 8 m thick; and massive upward-fining coarse to medium-grained sandstone up to 1.5 m thick. Laterally continuous thinly and thickly interbedded tabular sand- and mudstones form numerous upward-

fining successions tens of meters to hundreds of meters thick. The organic-rich finer-grained fraction (very fine sandstone, mudstone and shale) makes up approximately 60 % of the section. Mudstone and carbonaceous shale range in thickness from a few cm to more than 14 m and locally contain thin seams (<10 cm) of coal and interbedded bentonite (Fig. 3). We also recorded intercalated, sharp-based non-structured deposits that incorporate clasts and woody debris in a fine-grained organic-rich matrix. Rocks are well-indurated, have a dark grey to black color, and commonly preserve primary bedding features. In a few places, beds are truncated by dikes and interleaved by sills.

Dominant sedimentary features include muddy partings in sandstone and conglomerate, trough cross-bedding, current ripples, and soft-sediment deformation. Channel scour is rare (Tomsich et al., 2010). Paleoflow measurements record bimodal directions (SE and NW) in near equal proportions.

Geochronological Analyses

The weighted mean or best fit U–Pb zircon ages for two bentonites from Sable Mountain yielded 71.5 ± 0.9 Ma and 71.0 ± 1.1 Ma ages, respectively. For the lower bentonite (Bentonite 1), a total of 60 zircon grains were analyzed of which 54 grains yielded concordant results. Eleven grains yielded ages older than the probable age of the Cantwell Formation (based on the biostratigraphy of Ridgway et al., 1997), and 3 failed to pass an applied error filter set at 10%. Of the remaining 40 grains, two more were rejected at the 95% confidence level (shown as blue bars in the histogram; Fig. 4a). The age span for the older grains ranges from 195.3 to 2556.8 Ma. These grains are considered detrital zircons that were either incorporated into the ash during magma ascent and/or were sourced from the sedimentary environment. Ages for the remaining zircon grains, for which the weighted mean age was constrained, range from 64.57 to 80.06 Ma (Fig. 4a). U/Th ratios, a discriminator for the source rock type, range from 1.06 to 3.42 with an average of 2.09 (Appendix A, Table A-1), which suggests that all zircon grains are igneous-sourced (see Hoskin and Schaltegger, 2003). For the upper bentonite (Bentonite 2), a total of 60 zircon grains were scanned. Twenty-eight grains yielded ages older than the probable stratigraphic

Table 2. Paleomagnetic results for lower (this study) and upper Cantwell Formation (Sontag, 1992). Application of a mean flattening factor (see Kent and Irving, 2010) yielded a plausible paleolatitude of 63.3° N for the sedimentary rocks. Paleomagnetic data from Sontag (1992) presented here for comparison consistently gave high inclinations yielding a mean paleolatitude of 74.3° ± 6° N and paleopole of 177° E, 75° N for ~ 60–58 Ma volcanic strata near Polychrome Mountain. Polarity is reversed in all samples.

Sample Location	Geographic Coordinates	Approx. Age (Ma)	DeMag step	Intensity (mA/m)	GeoDec	GeoInc	StratDec	StratInc	2 σ	Paleo-latitude	Notes
Sable Mountain	63.6/-149.45	~ 72	NRM	0.187601	108.9	78.6	330.9	9.6			This study
			NRM after liquid nitrogen	0.098443	119.8	42.6	5.2	25.8			
			10 mT AF	0.088212	355.4	-30.2	149.7	-65.4		47.5	
Polychrome Mountain		59.8 ± 0.2								Sontag, 1992	
North limb 1	63.6/-149.6				153	-45	149	-68	13.1		
North limb 2					167	-40	185	-71	7.2		
North limb 3					174	-41	193	-62	3.3		
North limb 4					178	-57	224	-73	26.9		
North limb 5					157	-43	142	-64	2.1		
North limb 6					154	-51	132	-71	2.1		
North limb 7					169	-47	341	-85	13.6		
North limb -- Mean					164	-47	169	-74	11.1		
South limb 1	63.5/-149.6				32	-41	73	-79	5.9		
South limb 2					22	-52	184	-87	40.7		
South limb 3					20	-45	141	-81	2.8		
South limb 4					22	-40	29	-75	28.8		
South limb 5					39	-46	84	-75	6		
South limb 6					25	-48	337	-89	9.1		
South limb 7					31	-44	126	-76	5.5		
South limb 8					25	-33	73	-77	2.5		
South limb -- Mean					27	-44	86	-82	6.1		
East Toklat Ridge	63.5/-149.55	57.8 ± 2.7	n/a	n/a	127	-39	156	-53	5.4		Sontag, 1992
East Toklat Ridge					84	-47	65	-69	19.8		
East Toklat Ridge					98	-63	158	-75	4.4		
East Toklat Ridge					110	-68	327	-88	4.5		
East Toklat Ridge					125	-51	253	-75	41		
East Toklat Ridge					137	-46	231	-71	9.2		
East Toklat Ridge					94	-50	109	-82	21.8		
East Toklat Ridge					106	-57	192	-85	3.1		
East Toklat Ridge-- Mean					111	-54	166	-82	12.3		
Polychrome Mountain-- Mean	63.5/-149.6	~ 60 – 58			98	-64	149	-82	2.3	74.3 ± 6	Sontag, 1992

age, 2 grains yielded ages <60 Ma, 5 grains failed to meet concordance tests and 2 grains failed to pass the 10% error limit. Of the remaining 23 grains, one more was rejected at the 95% confidence level (Fig. 4b). The older grains range in age from 81.8 to 2595.4 Ma and are likely detrital in nature. Ages for the remaining zircon grains ranged from 67.53 to 77.91 Ma yielding a weighted mean age of 71.0 ± 1.1 Ma at the 95% confidence level (Fig. 4b). U/Th ratios vary from 0.61 – 5.30 (Appendix A, Table A-2) with an average of 2.32, indicating that all are igneous-sourced.

Fossil Fauna of the Lower Cantwell Formation at Sable Mountain

The most important fossil vertebrate information for the lower Cantwell Formation is derived from

the ichnofossil record. Only a few poorly preserved bone fragments have been recovered to-date; thus, well-preserved vertebrate tracks play an important role in the reconstruction of faunal communities. Dinosaur tracks have been found in coarse-grained facies but are relatively common in the finer-grained, heterolithic facies of the lower Cantwell Formation. Many well-defined footprints are preserved as casts (Figs. 5 and 6) at a depositional break. Moreover, numerous small to large bulbous load casts have weathered out on the underside of more resistant beds. It is not uncommon for two or more tracks to form a short trackway along the bottom of a more resistant sandstone bed from which stride and mode of locomotion is determined and hip heights may be estimated (see Wright and Breithaupt, 2002). The majority of the dinosaur tracks in the Sable



Fig. 5. Hadrosaur footprints and manus print (above hammer) on underside of inclined bedding plane. Foot length is 32 cm. This translates into an ornithischian hip height of ~ 1.9 m (after Wright and Breithaupt, 2002). Tracks are of inferred late Campanian age. Hammer is 42 cm long.



Fig. 6. *Saurexallopus* sp., a therizinosaur footprint (Fiorillo and Adams, 2012). The 23 cm long and 20 cm wide track occurs above Bentonite 2 and is of inferred early Maastrichtian age. Form and age are comparable to *Saurexallopus lovei*, a therizinosaur footprint from the Maastrichtian of northwestern Wyoming. Similar tracks were reported from Poland implying a wide biogeographic range. Scale bar = 5 cm.

Mountain area are underprints and the variability of preserved detail is likely related to floodplain dynamics (Jackson et al., 2009). A few exquisitely preserved tracks exhibit evidence for direct contact with the sediment, such as those with distinctive impressions of foot skin tubercles.

Five Late Cretaceous dinosaur groups have been recognized from the track record. They are attributable to theropods (including birds and therizosaurs), hadrosaurs (duck-billed dinosaurs, Fig. 5), ceratopsians (horned dinosaurs) and ankylosaurs (club-tail dinosaurs). Hadrosaur tracks are the most abundant and vary in length from 10 to 60 cm, with ceratopsian tracks being the next most common. Definitive tracks attributable to ankylosaurs are rare.

Non-avian three-toed theropod tracks are

small to medium-sized; the largest footprint of this predatory dinosaur group found to-date at Sable Mountain is 25 cm long. Recent discoveries include the four-toed tracks of a therizinosaurid dinosaur (Fig. 6), an unusual herbivorous theropod (Fiorillo and Adams, 2012). Tracks and body fossils of this enigmatic group of animals are found in Asia and North America (Harris et al., 1996), and contribute to the model of faunal exchange between these two continents during the Late Cretaceous (Fiorillo, 2008; Fiorillo and Adams, 2012).

Avian dinosaur tracks include seven types of bird tracks and probable feeding traces (Fiorillo et al., 2007; 2011). Track sizes range from small wading shore bird traces to large tracks (Fig. 7) comparable to a sandhill crane (*Grus canadensis*). The morphology of the smaller traces is similar to the tracks of a willet



Fig. 7. *Magnoavipes denaliensis*, a new ichnospecies (Fiorillo et al. 2011) dated to 71.5 ± 0.9 Ma. Shown are three well-defined bird tracks and one overlapping faint bird trace (arrow). The well-defined tracks preserved toe pad detail. Imprinted medium is a bioturbated, laminated siltstone interpreted as lake margin sediment. Unidirectional track orientation indicates that the birds moved as a group. Prints are 25 cm long and compare in size and form to those of sandhill cranes. Card shown for scale is 8.5 cm long.

(*Catoptrophorus semipalmatus*) or a sand piper (*Actitis hypoleucos*). Two new ichnospecies were established on account of detailed morphological features that distinguish them from those previously described under the same ichnogenus. Alluding to their size, Fiorillo et al. (2011) named the smallest tracks *Gruipeda vegrandiunus* and, alluding to Denali, North America's highest mountain, Fiorillo et al. (2011) called the largest tracks, found at Sable Mountain just above Bentonite 1, *Magnoavipes denaliensis* (Figs. 3 and 7).

Four-toed ornithischian footprints record the presence of either ceratopsian dinosaurs (e.g., triceratops) or ankylosaurs, or both, as the hind tracks of these quadrupedal animals are indistinguishable from one another and skeletal remains of both groups have been identified from Late Cretaceous bone fossil localities of Alaska. Skeletal parts and skulls of several ceratopsids (e.g., *Pachyrhinosaurus perotorum*; Fiorillo and Tykoski, 2012) were recovered from the coeval Prince Creek

Formation on the North Slope, and the skull of a dermal armor-plated ankylosaur (*Edmontonia longiceps*) was unearthed from the Maastrichtian Matanuska Formation of southern Alaska (Gangloff, 1995; Fiorillo, 2006).

Non-dinosaurian vertebrate ichnofossils include fish fin traces (*Undichna*) and pterosaur manus prints (Fiorillo et al., 2009a). In reference to the Cretaceous paleopole, the pterosaur tracks from Sable Mountain are the northernmost documentation to-date for this unusual, extinct reptile group. Their habitat evidently extended inland suggesting rich fishing grounds for the Cantwell basin as this group would have fed primarily on fish (Fiorillo et al., 2009a).

Invertebrate trace fossils occur mainly at or just below a depositional break and, although not abundant, are quite diverse (Fiorillo et al., 2009a; Hasiotis, 2009, 2011). They include back-filled burrows made by mud-burrowing beetles (*Steinichnus*; Hasiotis et al., 2009, 2011), U-shaped

burrows of fly larvae (c.f. *Arenicolites*), crayfish burrows (*Camborygma*), and intricate ostracod (*Sagitichnus*), freshwater gastropod (*Scolicia*; cf. *Isopodichnus*), and other subsurface grazing trails (e.g., *Mermia*; Hasiotis, 2002). Sinusoidal traces (*Cochlichnus* sp.) attributable to nematodes and oligochaetes were imprinted at the sediment–water interface of standing water bodies as were microbial matting patterns. Also found were subaerial beetle trackways, channelized fossil wood (*Paleobuprestos*) from which we infer the presence of wood-burrowing beetles (S. Hasiotis, pers. comm.) and minor leaf fossil evidence for insect herbivory.

Fossil Flora of the Lower Cantwell Formation at Sable Mountain

The lower Cantwell Formation contains abundant plant impression and compression fossils and lithified wood. A total of 42 species were counted from the Sable Mountain study area. Gymnosperm fossils consist of conifer leaves, leafy shoots, cones (Fig. 8), seeds, sideritized wood, and tree bark and trunk impressions up to 2.5 m long. Leafy shoots of deciduous conifers of the family Cupressaceae

are abundant and are identified as *Taxodium* sp., *Metasequoia* sp., *Glyptostrobus* sp., possible *Parataxodium* sp., and *Sequoia*-like forms. Other conifers resemble *Tumion* (*Torreya*), a member of the Taxaceae, and the form genera *Cephalotaxopsis* and c.f. *Pityophyllum* of unknown affinities (Tomsich et al., 2010). Needles, isolated or in bundles, and cones (Fig. 8) referable to piceoid conifers (e.g., *Pinus*, *Larix*, and possibly *Picea*) were also observed, albeit less frequently. The low abundance of these taxa could signify that they retained their foliage for several years or that they grew outside the locus of deposition.

Dicot angiosperm leaf fossil impressions consist of simple entire and simple lobate leaf forms and include the following taxa: *Corylites beringianus* (Krysht.) Moiseeva, *Corylites* sp., and other betulaceous taxa; *Celastrinites* (*C. kundurensis?*); and hamamelidaceous, nymphaeaceous (cf. *Nuphar*) and platanoid taxa. The latter include *Pseudoprotophyllum* sp., *P. boreale*, *Platanites* sp., and several other platanoids of unclear generic affinities. Palmate-acrodromously veined leaf forms are assigned to *Menispermites*



Fig. 8. Longitudinal section of piceoid conifer seed cone showing hollow center axis and ovuliferous scales. Fossil is embedded in gritty siltstone interpreted as a mud flow. Scale bar = 1 cm.

sp., *M. septentrionalis*; *Trochodendroides* sp. 1,2, *T. richardsonii*, *T. taipinglinchanica*; and *Macclintockia* sp. Three additional morphotypes, including one aquatic? angiosperm leaf form resembling Trapago and another resembling *Ulmus-Zelkova*, remain unidentified due to poor preservation of higher-order venation.

The plant fossil collection also includes magnoliid seeds, several linear (*Phragmites*- and *Typha*-like) and broad-leaved (*Potamogeton*- and *Alisma*-like) monocot angiosperm taxa, the fern genera *Asplenium*, *Cladophlebis*, *Coniopteris*, and *Gleichenites*, mosses (*Lycopodium*), and abundant horsetail (*Equisetites*) stems and rhizomes of varying diameter and segment lengths (Tomsich et al., 2010). Ginkgophyte and cycadophyte leaf fossils are suspiciously absent in our study area, but have been observed elsewhere. For example, we noted Ginkgo leaves (e.g., *G. adiantoides*) from outcrops in the northwestern Cantwell basin and cycadophyte material from Double Mountain and at an outcrop above the East Fork Toklat River. *Ginkgo* leaves and *Nilssonia yukonensis* were also reported from the base of the Cantwell Formation east of the Nenana River (Alaska Paleontological Database, 2014).

Plant fossil assemblages differ in composition across the Cantwell basin because they reflect climate variability through time, various stages of floral successions, or various local depositional parameters. Distinctive plant communities appear to have been endemic to specific sedimentary subenvironments, likely for edaphic reasons. Accordingly, a *Taxodium*—*Glyptostrobus*—*Alnites* assemblage is associated with poorly-drained fine-grained floodplain sediments, and a *Metasequoia*—*Corylites*—*Trochodendroides* assemblage is associated with more heterogeneous and better-drained floodplain deposits. These mixed conifer and broad-leaved angiosperm leaf fossil assemblages commonly also include ferns and horsetails and contrast starkly with platanoid-dominant leaf assemblages found in what we interpret as channel and overbank deposits and a low-diversity community of *Equisetites* and cycadophytes observed at Double Mountain for which we infer growth in a marshland.

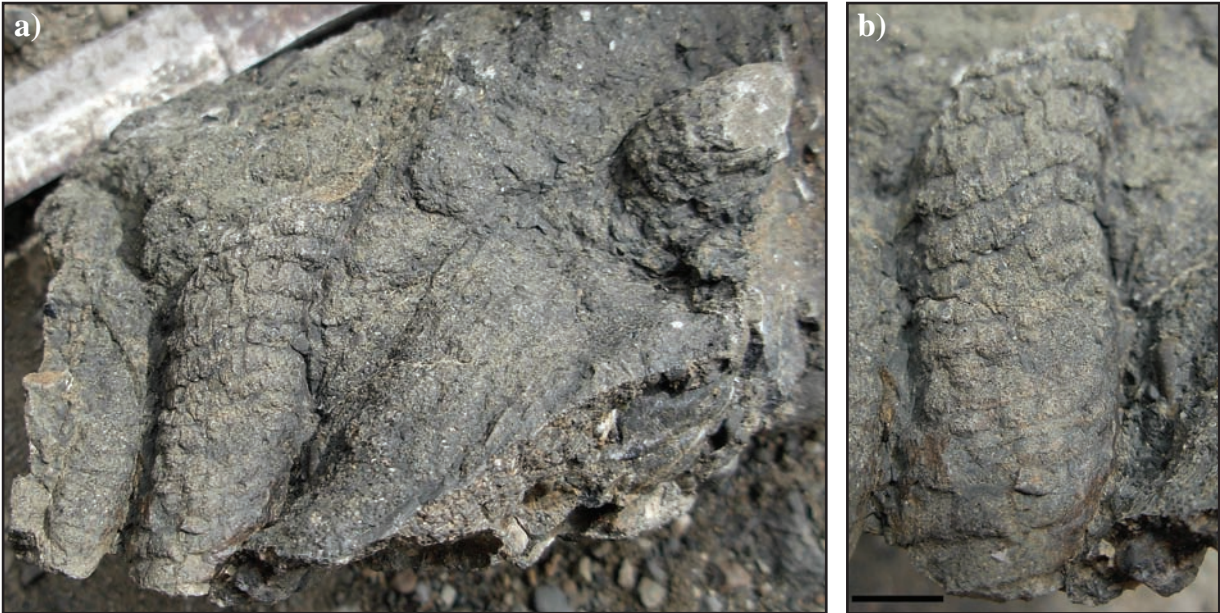
The generic taxonomy of the Sable Mountain flora shows a strong similarity to the late Maastrichtian Koryak flora of northeastern Russia

(Tomsich et al. 2010). It also partly overlaps the Campanian–Maastrichtian Hanson Point flora from Ellesmere Island in the Canadian Arctic Archipelago (Falcon-Lang et al., 2004), the Edmonton flora of the central Alberta Foothills described by Bell (1949), and older floras such as the Cenomanian (and Turonian?) Melozi and Kaltag Formation floras of the Yukon River basin (Hollick, 1930; Patton et al., 1994). Taxa are characteristic of a Pan-Beringian flora, the Late Cretaceous–early Tertiary polar broad-leaved deciduous forest. This unique fossil flora was characterized by a prevalence of deciduous conifers and angiosperms of low familial diversity (Wolfe, 1987; Spicer et al., 1987; Herman, 2007; Krassilov et al., 2009; Spicer and Herman, 2010). Woody angiosperms exhibit a high degree of polymorphism and speciation (Spicer and Herman 2010). Herbaceous angiosperms may have been present also, but are not preserved except in the pollen record and, possibly, in form of root casts (as shown in Fig. 9). Casts and impressions of tree trunks no more than 10 cm in diameter indicate that woody angiosperms had a shrub-like habit. Conifer tree trunk diameters, on the other hand, vary from 25 cm to an estimated 1 m or more at the base. Several trunk impressions may indicate buttressed bases (Fig. 10).

The taxa listed above constitute the principal floodplain vegetation in the Sable Mountain area. The relative abundance of deciduous cupressaceous conifer fossils suggests that members of this family were dominant in this part of the basin. Rare detached, pine-like conifer needles indicate they were only minor constituents of the floral community. However, a pinaceous seed cone embedded in a gritty siltstone (Fig. 8) suggests that it, too, was in situ.

Paleoclimatic Reconstruction of the Lower Cantwell Formation at Sable Mountain

The Late Cretaceous high-latitude (>65° N) terrestrial faunal and floral fossil data record species expansion in a habitat governed by a temperate climate and polar light regime (Wolfe, 1987) which may have led to unique adaptation strategies. Dinosaur egg shell fragments (Godefroit et al., 2009), juvenile dinosaur bones (Clemens, 1994; Gangloff and Fiorillo, 2010; Fiorillo et al., 2010) and small, possibly juvenile hadrosaur footprints suggest



Figs. 9 a), b). Tuberos roots cast in coarse-grained granular sandstone. 9a) Cluster of tubers. Hammer shaft for scale is 2 cm wide. 9b) Single tuber, enlarged. Scale bar = 1 cm. Although probably of little taxonomic value, we report this fossil for its evolutionary and paleoclimate implications. Selection for asexual reproduction may have been an adaptive response to short growing seasons and suggests a frost-free substrate.



Fig. 10. Conifer tree trunk impression 2.5 m long (arrows) in inferred rapidly aggraded channel deposits of Campanian age. Tree base diameter is estimated at >1 m diameter and appears buttressed. Note the shallow spread of the root system which suggests a wet floodplain. Person for scale.

that environmental conditions were sufficiently hospitable for dinosaurs to remain year-round (see also Fiorillo and Gangloff, 2001; Chinsamy et al., 2012). Being sessile, plants are genetically coded to cope with climate, low-light settings, and surface boundary interactions. For example, tuberous root casts (Fig. 9), tree trunk impressions and casts (Fig. 10), and lithified wood provide a glimpse into the boreal forest structure that has been considered one of the causes of amplified polar warming (Otto-Bliesner and Upchurch, 1997; Upchurch et al., 1998). Woody dicot leaf physiognomies are important paleoclimate proxies because leaves are highly sensitive to, and therefore responsive to, climate and insolation (Wolfe and Spicer, 1999; Spicer and Herman, 2010).

A paleoclimate analysis (Climate Leaf Analysis Multivariate Program or CLAMP for short) for 19 dicotyledonous angiosperm leaf fossil types yields a mean annual temperature (MAT) of $7.4 \pm 1.2^\circ\text{C}$, a warmest monthly mean temperature (WMMT) of $17.1 \pm 1.6^\circ\text{C}$ and a coldest monthly mean temperature (CMMT) of $-2.3 \pm 1.9^\circ\text{C}$ (Tomsich et al., 2010). Growing season precipitation is estimated at $229 \pm 336\text{ mm}$, and the length of the growing season is estimated at 4.8 ± 0.7 months. The annual temperature range is $19.4 \pm 3.5^\circ\text{C}$ (Table 3). Results indicate a cool temperate, highly seasonal paleoclimate. Closely spaced and well-pronounced tree rings in fossil conifer wood suggest short, rather abrupt-ending growing seasons. The reduction of sunlight in late summer likely limited annual growth (Tomsich et al., 2010).

Growing season precipitation is rather low compared to other Maastrichtian sites (Table 3), but precipitation estimates have a large error margin likely because of missing data that codes for precipitation such as the leaf apex on the larger-sized leaf fossils (Spicer et al., 2005; Tomsich et al., 2010). However, if the low precipitation estimate for the growing season is valid, it could have important implications for the paleographic setting. Tree diameter size, leaf size and the occurrence of tuberous root casts (Fig. 9) also have important climate implications and are discussed below.

DISCUSSION

Depositional Environments at Sable Mountain

The Sable Mountain lithofacies (Table 1) are

characterized by a mix of fine-grained and coarse-grained facies that correspond largely to facies association (FA) 2, 3 and 4 of Ridgway et al. (1997).

On an alluvial fan, sediment grain size decreases sharply with increasing distance from the fan apex (Ridgway et al., 1997; Kumar et al., 2007). From the high proportion of fine-grained facies (60% of very fine sandstone or finer), we infer a medial to distal location for the site of deposition. We interpret the matrix-rich, non-stratified gravelly facies (F 1) as debris flow and the predominantly massive matrix-supported clast-conglomerates (F 2) as gravelly stream deposits that accumulated rapidly under hyper-concentrated flow conditions in non-channelized gravelly stream beds and flood channels (Blair and McPherson, 1994; Miall, 2006; Kumar et al., 2007). Deposition may have been triggered by a storm or flood event and was facilitated by steep alluvial slope angle and high sediment to water supply ratio (Wells and Harvey, 1987). In contrast, stratified conglomerate (F 3), cross-stratified pebbly sandstone (F 4), and thick massive, cross-bedded or horizontally stratified sandstone (F 5, F 6) are interpreted as in-channel traction flow deposits (Miall, 2006) with the lesser-organized facies being transitional to dilute flow (Wells and Harvey, 1987). Thick sandstone deposits up to 8 m high (F 6) represent amalgamated multistory sandy channel fill. Main flow direction was to the south. However, north-directed paleocurrent measurements from cross-stratified conglomerates along the southern part of the study area suggest interfingering deposition by a sinuous axial river.

Laterally continuous tabular sandstone beds up to 1 m thick are inferred to be sheetflood deposits (F 7, F 8). Numerous depositional breaks, reactivation surfaces, stringers of mudstone, lateral continuity of beds and the near-absence of scour marks imply unconfined sheet-flow under a flash-flood discharge regime and changes in sediment influx (Bull, 1977; Miall, 2006). Mud drapes indicate waning flow and flow abandonment. Lush floodplain vegetation may have significantly slowed currents thus promoting deposition on the fan (Bull, 1977).

Fine to very fine sandstone (F 9) and interbedded sandstone and mudstone (F 10) were deposited under waxing and waning flow stages during overbank flow. These facies associations

Table 3. Paleobotanical climate estimates for the lower Cantwell Formation flora at Sable Mountain and other Maastrichtian floras of North America and northeastern Russia. Results from Parrish et al. (1987); Spicer and Parrish (1990a); Golovneva (1994; 2000); Moiseeva (2005); Spicer and Herman (2010), Tomsich et al. (2010) and Flaig et al. (2013). Estimates for the Cantwell, Kakanaut, Sakhalin Island and Alberta floras were obtained from CLAMP. Uncertainties represent 2 sigma deviations of the residuals about the calibration regressions. Estimates for the Koryak flora and the Chignik flora were obtained from LMA. Temperature variables for the Prince Creek Formation were extrapolated from a latitudinal temperature curve and the floristic composition; precipitation estimates were obtained from stable isotope analyses. Paleolatitudes were approximated from paleopole positions using the Maastrichtian (70 Ma) mean pole and 2-sigma confidence level of Enkins (2006, in Kent and Irving, 2010).

Formation, Locality (Present Latitude)	Age (Ma)	Paleo-Latitude (°N)	Mean Annual Temperature (C°)	Warmest Monthly Mean Temp. (C°)	Coldest Monthly Mean Temp. (C°)	Length of Growing Season (Months)	Mean Annual Precipitation (mm)	Growing Season Precipitation (mm)	Three Driest Months Precipitation (mm)
Cantwell Sable Mtn. S.-central Alaska (63.5°N)	~ 72	~ 70 ± 5	7.4 ± 2.4	17.1 ± 3.2	-2.3 ± 3.8	4.8 ± 1.4	n/a	229 ± 672	141 ± 186
Prince Creek Northern Alaska (70°N)	~ 70	80 ± 5	2.5 – 6	10 – 12	2 – 4	n/a	500-1500	n/a	n/a
Koryak NE Russia (63°N)	Mid- to late Maastrichtian	75 ± 5	3 – 4	n/a	n/a	n/a	n/a	n/a	n/a
Kakanaut NE Russia (63°N)	Mid- to late Maastrichtian	75 ± 5	10	19	3	6.3	1414	948	181
Sakhalin (49°N)	Maastrichtian	56 ± 5	14	20	8	8	1892	1214	293
Chignik, Chignik Bay (56°N)	Late Campanian to early Maastrichtian	~ 60 ± 5	11 – 13	n/a	n/a	n/a	n/a	n/a	n/a
Edmonton Group, Alberta, Canada (53°N)	Mid- Maastrichtian	54 ± 5	12	19	5	7.1	1804	1586	335

include thick successions of thinly interbedded sand- and mudstones and small channel sandstone bodies that are indicative of distal crevasse splay complexes. Laterally extensive siltstone and thinly bedded sandstone–mudstone couplets typify levee and floodplain deposits, respectively.

Shale and laminated mudstone (F 11, F 12) are inferred to have accumulated in abandoned

channel beds, on inactive channel bars, on the floodplain, and in marginal well-drained lacustrine environments. Carbonaceous mudstone and coal (F 13, F 14) are inferred to have accumulated in poorly drained stagnant backwater swamps. These low-energy environments also preserved Late Cretaceous pyroclastic fall-out suspension deposits that altered to bentonite (F 15). Gritty siltstone accumulations

(F 16) are interpreted as mud flows. Lastly, igneous intrusive rocks (F 17) formed of near-surface basaltic lava flows in the Latest Cretaceous and Tertiary. The microcrystalline texture of a few small plugs could indicate significant burial depths.

Overall, the dark color of the rocks and minimal post-depositional sediment modification imply that the depositional environments were saturated most of the time. The lateral discontinuity of the beds, numerous depositional breaks and facies changes, an extremely low channel inter-connectedness, and predominantly matrix-supported stream-flow and gravity flow deposits are all architectural elements of wet alluvial fan systems (Bull, 1977; Wells and Harvey, 1987; Blair and McPherson, 1994; Talling et al., 1995; Miall, 2006; Kumar et al., 2007). Strongly bimodal (NW and SE) paleocurrent directions suggest frequent shifting of sinuous channels possibly as a result of periodic basin margin uplift and load-induced subsidence (Talling et al., 1995). From the large fraction of finer-grained facies, the sandstone sheets and the evidence for vertically aggraded channel sandstone deposits with a total width in excess of 150 m, we conclude that the locus of deposition was near the basin axis and entailed the following subenvironments located in close proximity: distal alluvial fan (including gravelly braided and sandy braided distributary channel, flood channel and sheet flow, alluvial slope floodplain and lacustrine settings), fan toe, and possibly interfingering axial river and alluvial floodplain deposition (Tomsich et al., in prep.).

Clast identification and petrographic analyses (Trop and Ridgway, 1997; Tomsich et al., in prep.) reveal a polymictic lithology derived from greenschist metavolcanic and plutonic rocks, greenschist-facies metasedimentary rocks, tectonite, chert, argillite, limestone, and reworked lower Cantwell Formation. Detritus was sourced from uplifted basin margins, mountainous hinterland and eroding intrabasinal highs. Trop and Ridgway (1997) showed that sandstone modal compositions vary greatly across the basin, which they attribute to the complexity of a collaged suture zone and uplifted plate margins. Source-diagnostic discrimination diagrams (Dickinson et al., 1983, Zahid and Barbeau, 2012) indicate a recycled orogen and a dissected magmatic arc (Trop and Ridgway, 1997; Tomsich et

al., in prep.).

Implications of New Numerical Ages for the Lower Cantwell Formation

Present research on the lower Cantwell Formation in Denali National Park and Preserve (Salazar Jaramillo et al., in prep. and this study) has provided the first numerical ages for the formation. Our U–Pb zircon ages of 71.5 ± 0.9 Ma and 71.0 ± 1.1 Ma for two bentonites separated by 24 m of section at Sable Mountain are within error of each other and therefore, constitute very robust data. Our results place the bird ichnospecies *Magnoavipes denaliensis* of Fiorillo et al. (2011) (Fig. 7) at and the pterosaur manus track near 71.5 ± 0.9 Ma and permit relative age determinations for all other strata. In 2012, the International Commission on Stratigraphy (ICS) placed the Campanian / Maastrichtian boundary at 72.1 Ma (Walker et al., 2013). Accordingly, the Sable Mountain deposits straddle this important boundary, which is marked by significant global cooling and sea level fall (Hay, 2008). The age of the basal section above the Sable Mountain fault is therefore Campanian, and most likely late Campanian. Correspondingly, the upper part of our section (not shown in Fig. 3) is likely of Mid-Maastrichtian age or younger. All dinosaur footprints at Sable Mountain are now interpreted to be of both upper late Campanian and early Maastrichtian age with the majority occurring in the former, provided that all beds of our composite section are in sequential order (e.g., not duplicated by blind thrust faults). Moreover, we consider the age of the plant fossil data used for a paleobotanical climate analysis (CLAMP; Tomsich et al., 2010) earliest Maastrichtian. The Sable Mountain exposures containing the bentonites correlate with upper strata at Polychrome Mountain, which were dated by Ridgway et al. (1997) to the early Maastrichtian based on the occurrence of the stratigraphically restricted pollen taxon *Kurtzipites andersonii*. This taxon ranges from 72.5 to 71.1 Ma according to biostratigraphic zonations determined for the Canadian basins (Braman and Sweet, 2012).

Outside the Cantwell basin, the lower Cantwell Formation at Sable Mountain correlates well in time with the Campanian–Maastrichtian Prince Creek Formation on the North Slope of Alaska and the Chignik Formation of southwestern Alaska. Further

away, more chronostratigraphic correlations can be made with the upper Bonnet Plume Formation in Yukon Territory, Canada, which has also yielded avian fossils (Rich et al., 2002), the upper part of the marine East Fork and the Summit Creek formations of the Brackett Basin in the Northwest Territories (Sweet et al., 1989; Braman and Sweet, 2012), the plant fossil beds of the Hanson Point Volcanics at Emma Fjord, NW Ellesmere Island in the Canadian Arctic (Falcon-Lang et al., 2004), the Horseshoe Canyon Formation in southern and central Alberta and the St. Mary River Formation of southwestern Alberta (Braman and Sweet, 2012), all of which straddle the Campanian/Maastrichtian boundary. Across the Bering Sea, the lower Cantwell Formation at Sable Mountain is partly correlative to Campanian plant megafossil-yielding strata of the Kundur Formation (Golovneva et al., 2008) and the late Campanian and early Maastrichtian dinosaur fossil-bearing strata of the Kundur and lower Udurchukan formations in the Amur River region of eastern Russia (Van Itterbeeck et al., 2005).

Assessing the Paleomagnetic Data

Our paleomagnetic sample from Sable Mountain shows sufficient remanence after demagnetization and an inclination of -65.4° indicating a reverse polarity. This reversal can be used to help define the age of the section. The new numerical age constraints reveal that the Sable Mountain section correlates to Magnetochrons 31 and 32. Lerbekmo and Braman (2005) used densely spaced paleomagnetic inclination measurements from the Canadian Pacific Oil and Gas Strathmore (CPOG) well core to identify eleven reversals in Magnetochron 32 (seven in Subchron 1 and four in Subchron 2) in the late Campanian Bearpaw and latest Campanian to early Maastrichtian Horseshoe Canyon formations. Our sample is consistent with deposition during one of the Chron 32 reversals. More paleomagnetic data are needed to determine the reversal stratigraphy and paleopole position for the lower Cantwell Formation.

In contrast to the sedimentary samples, the volcanic rocks of the Paleocene upper Cantwell Formation gave consistently high paleomagnetic inclinations (Sontag, 1992). The mean paleomagnetic pole is 177° E longitude and 75° N latitude with an

average error of 10.4° at the 95% confidence level. This result matches the position for the 120 to 60 Ma relative still-stand of the paleopole for North America (193.9° E, 76.2° N $\pm 1.6^\circ$) (see Kent and Irving, 2010) with fully overlapping circles of 95% confidence. The calculated paleolatitude for the composite volcanic sample set is $74.3^\circ \pm 6^\circ$ (Table 2; also see Sontag, 1992). Since Sontag's study, the volcanic rocks have been dated, using K–Ar, to 58.7 ± 3.5 Ma (Csejtey et al., 1992) at or near the East Fork sample site and, using $^{40}\text{Ar}/^{39}\text{Ar}$, to 59.8 ± 0.2 Ma (Cole et al., 1999) at or near the Polychrome paleomagnetic sample site. Thus, the maximal difference between the new numerical ages at Sable Mountain and Sontag's samples is approximately 13.3 ± 4.4 Ma. Northwestward displacement of 450 km along the Tintina Fault during the latest Cretaceous and earliest Tertiary (Till's et al., 2007b) would result in approximately 2 - 3° of latitude difference between the lower and upper Cantwell Formation. This translates into the lower Cantwell Formation being within a few degrees north of its present location during the Late Cretaceous.

Age of Plant Fossils and Paleoclimate Implications

Fluctuating climates leading up to the Cretaceous terminal event and the demise of many of the ecological groups that lived therein, have produced a mosaic of late Cretaceous biogeographic species distribution, ecosystems, and species radiation. While immediate effects of these oscillations are still being evaluated, data recovered to-date have been applied to model the complex interactions between land surfaces, oceans, atmosphere and biosphere of the past. These models depend heavily on accurate, high-resolution paleoecological information from different paleogeographic regions. Much insight can be gained from the comparison of co-eval sites that were subjected to similar conditions.

The new numerical ages allow us to surmise that the Sable Mountain florule used for the paleobotanical climate analysis (Table 3) (Tomsich et al. 2010) date to ~72 to 71.5 Ma or earliest Maastrichtian. This was a time marked by the onset of significant cooling as suggested by marine isotope data (Frakes, 1999; Zakharov et al., 1999; Hay, 2008; Zakharov et al., 2011). Thus, the MAT of $7.4 \pm 2.4^\circ$ C, a WMMT of $17.1 \pm 3.2^\circ$ C and a CMMT

of $-2.3 \pm 3.8^\circ\text{C}$ calculated for the Sable Mountain flora corresponds to this cooling trend (Table 3). Our temperatures are cooler than temperature estimates for the mid-to-late Maastrichtian Kakanaut flora of the Koryak Uplands located at a paleolatitude of 70 to 75°N (Godefroit et al., 2009), but warmer than estimates for the coeval Prince Creek Formation (~ 2.5 to 6°C ; Spicer and Parrish, 1990a; Herman and Spicer, 2010; Flaig, 2010; Flaig et al., 2013), which are based on a polar temperature curve for paleobotanical climate data of lower latitudes and on comparative analyses for conifer tree ring growth characteristics (Spicer and Parrish, 1990a,b; Spicer, 2003). They are also warmer than a MAT of 3 to 4°C obtained for the mid to late Maastrichtian Koryak flora from a Leaf Margin Analysis (LMA) (Golovneva, 2000a; Herman et al., 2009). They are significantly lower than a MAT of 12°C estimated for the Maastrichtian Edmonton flora (see Table 3 and Golovneva, 2000a). The Edmonton Group was deposited proximal to the Cretaceous Western Interior Seaway (CWIS) in west-central Alberta, Canada, at a paleolatitude of $\sim 54^\circ\text{N} \pm 5^\circ$ using the paleopole for North America of Enkins (2006; in Kent and Irving, 2010). However, our new numerical ages suggest that the Sable Mountain flora is somewhat older than the Edmonton flora. Winter temperatures below freezing (CMMT of $-2.3 \pm 3.8^\circ\text{C}$) have not been reported from any other Campanian–Maastrichtian CLAMP data set for the North Pacific region (Table 3), but are therefore in good agreement with an early Maastrichtian geologic age and the predicted cooling trend for this interval. They are also in good agreement with an observed absence of cycadophyte fossil material regarded by many researchers (e.g., Golovneva, 2000a; Spicer and Herman, 2010) as thermophilic and with an observed reduction for tree stump diameters and angiosperm leaf sizes in inferred Maastrichtian strata.

The $19.4 \pm 5.2^\circ\text{C}$ mean annual temperature range contrasts with 16°C estimated for the Kakanaut flora, and $\sim 10^\circ\text{C}$ for the Prince Creek Formation (Table 3). Continentality and higher elevation remain a plausible explanation for low winter temperature estimates and greater temperature ranges. Ridgway et al. (1997) identified a marine incursion from marine to brackish water dinoflagellate cysts in samples from Double Mountain that they tentatively

correlate with the Bearpaw Transgression (~ 74 to ~ 72 Ma; Braman and Sweet, 2012). The end of this transgressive cycle also coincides with a transition from deep marine to subaerial exposure along the coast of southern Alaska beginning at ~ 72 to ~ 71 Ma (Trop and Ridgway, 2007). The predicted early Maastrichtian global sea level fall of 40 m (Hay, 2008) could thus have increased continentality during that time.

Additional evidence for a mountainous terrain comes from modal lithic sandstone composition analyses (Dickinson et al., 1983; Zahid and Barbeau, 2012) for the lower Cantwell Formation (Trop and Ridgway, 1997; Tomsich et al., in prep.) and from sandstone detrital zircon age populations (Hults and Tomsich, unpubl. data). These data, which are discussed further below, indicate that the Cantwell basin was surrounded by moderate topography associated with the late Mesozoic plate convergence (Csejtey et al., 1992; Ridgway et al., 1997; Cole et al., 1999), a factor that would have had a profound bearing on the local climate and the ecosystem. The influence of topography on atmospheric boundary conditions and associated cooling effect has been shown, for example, by Markwick and Valdes (2004). If valid, the paleobotanical temperature estimates for the Sable Mountain flora are consistent with a seasonal and cool temperate, continental climate (Tomsich et al., 2010). A similar suggestion was made by Golovneva et al. (2008) for a comparison of the late Campanian floras of the Amur River region in the Russian Far East and Sakhalin Island. The flora of Sakhalin Island contains more thermophilic taxa and was influenced by a warm maritime climate.

Paleogeographic Implications

Subduction-related Late Cretaceous (~ 80 to 66 Ma) continental margin arc magmatism was widespread in southern, central, and western Alaska (Moll-Stalcup, 1994; Trop and Ridgway, 2007; Cole et al., 2007), resulting in the emplacement of Late Cretaceous to early Tertiary granitoid plutons on either side of the late Mesozoic suture zone (Csejtey et al., 1992) and significant deformation along an orogenic belt stretching from eastern Alaska to the Bering Sea (Moll-Stalcup, 1994, Foster et al., 1994; Trop and Ridgway, 2007; Till et al., 2007b).

Regionwide uplift prior to a period of Late

Table 3. Paleobotanical Climate Estimates from Upper Late Cretaceous Floras of North America and Northeastern Russia

Formation, Locality (Present Latitude)	Age (Ma)	Paleo-Latitude (°N)	Mean Annual Temperature (C°)	Warmest Monthly Mean Temp. (C°)	Coldest Monthly Mean Temp. (C°)	Length of Growing Season (Months)	Mean Annual Precipitation (mm)	Growing Season Precip. (mm)	Three Driest Months Precip. (mm)
Cantwell Sable Mtn. S.-central Alaska (63.5°N)	~ 72	~ 70 ± 5	7.4 ± 2.4	17.1 ± 3.2	-2.3 ± 3.8	4.8 ± 1.4	n/a	229 ± 672	141 ± 186
Prince Creek Northern Alaska (70°N)	~ 70	80 ± 5	2.5 – 6	10 – 12	2 – 4	n/a	500-1500	n/a	n/a
Koryak NE Russia (63°N)	Mid- to late Maastrichtian	75 ± 5	3 – 4	n/a	n/a	n/a	n/a	n/a	n/a
Kakanaut NE Russia (63°N)	Mid- to late Maastrichtian	75 ± 5	10	19	3	6.3	1414	948	181
Sakhalin (49°N)	Maastrichtian	56 ± 5	14	20	8	8	1892	1214	293
Chignik, Chignik Bay (56°N)	Late Campanian to early Maastrichtian	~ 60 ± 5	11 – 13	n/a	n/a	n/a	n/a	n/a	n/a
Edmonton Group, Alberta, Canada (53°N)	Mid-Maastrichtian	54 ± 5	12	19	5	7.1	1804	1586	335

Paleocene to Early Eocene intracontinental extension (Cole et al., 2007) is also suggested by petrographic data and detrital zircon ages for a sandstone from the basal section at Sable Mountain (Hults and Tomsich, unpubl. data). The majority of zircon grains are Precambrian in age. The oldest rocks of the Wrangellia Terrane are not older than Pennsylvanian (Nokleberg et al., 1994; Plafker and Berg, 1994). Zircons older than Pennsylvanian therefore were sourced from the Yukon Tanana Terrane exposed to the north and east. A ~69 Ma caldera in the Sixty Mile Butte area (Bacon et al., 1990) overlies the schist of the Yukon Tanana Terrane about 200 km to the east of our study site indicating that no intervening lithological unit existed at the time and the schist was at or near the surface. In the eastern part of the basin, lower Cantwell Formation overlies Proterozoic schist and a

~95 Ma pluton (Wolfe and Wahrhaftig, 1970). North of the Hines Creek Fault, upper Cantwell volcanic strata overlie Precambrian schist (Fig. 1; Csejtey et al., 1992). While the Cantwell basin remained at a low to moderate elevation as suggested by a marine excursion interpreted to coincide with the Bear Paw transgression (Ridgway et al., 1997), the landform surrounding the basin margin may have been one of uplands, if not highlands. Topographic basins like the Cantwell basin may have existed all around the orogenic belt, but little of the sedimentary fill was preserved (Foster and Igarashi, 1990; Foster et al., 1994).

Elevated regional topography is also assumed by climate modelers. To calibrate surface boundary conditions for their GCM, Sewall et al., (2007) model the early Maastrichtian topography of the

southern Alaska region in the range of 200 to 800 m with isolated areas of up to 1000 m. In their model, the lowland vegetation constitutes a mixed evergreen and deciduous forest. Upland vegetation is inferred to have been composed of closed canopy evergreen conifer forest; the paleolatitudinal position of this area is presumed to have supported evergreen habit (Sewall et al., 2007). To this end, some conifer taxa such as *Sequoia* and some members of the Pinaceae are thought to have had an evergreen habit (Golovneva and Herman, 1998). Although a small number of *Sequoia*-like leafy shoots have been observed in the Cantwell Formation, no evidence for secondary (multi-year) growth has been observed to-date on any fossil conifer shoots. Because evergreens are low-littering plants, it is not clear whether the small collection of *Sequoia*-like shoots and pinaceous needles and cones represent minor constituents of the floodplain/alluvial slope vegetation or whether these taxa preferred the drier soils outside the floodplain and fossil material was upland-derived. The piceoid seed cone shown in Fig. 8 is preserved in a thick gritty siltstone that could imply that the fossil was sourced from within the basin.

The apparent dominance of hydrophilic deciduous conifers in floodplain deposits, indications for weak pedogenic processes and ichnofossil evidence for standing water bodies could support a wet climate interpretation. However, this is not supported by the low precipitation estimate for the Sable Mountain flora (Table 3). A possible explanation for the discrepancy is that in Arctic environments, water take-up from the substrate is severely reduced from the lack of transpiration following leaf abscission in response to late summer light reduction (Spicer 2003). Coupled with an apparent absence or low distribution of evergreen plants, the floodplain would have remained saturated for many months. As high water tables and high sediment influx are adverse to deep-rooting plants, the composition of the floodplain flora was likely influenced by tolerance thresholds corresponding to autogenic factors not applicable to bordering uplands. Elevation is thus an important factor in the climate reconstructions.

The Late Cretaceous climate of central and southern Alaska may have been largely frost-free

at low elevations and supported a more diverse flora that included temperature-sensitive taxa during warm intervals while mountainous regions supported hardier, better adapted, but possibly less diverse plant groups. A diverse and superbly preserved flora from non-marine interbeds of the mostly marine Chignik Formation on the Alaska Peninsula, southwestern Alaska, was described by Hollick (1930). The Alaska Peninsula is part of the Peninsula Terrane, the western subterrane of the Wrangellia Composite Terrane. The Chignik Formation was deposited on the shelf and shoreline of a fore-arc basin and includes up to 600 m (at the type section at Chignik Bay) of coastal-plain and alluvial fan sedimentary rocks (Mancini et al., 1978; Detterman et al., 1996) which also yield dinosaur footprints (Fiorillo and Parrish, 2004). Non-marine palynomorphs and a molluscan fauna indicate a late Campanian to early Maastrichtian age (Mancini et al., 1978; Detterman et al., 1996). Thus, the Chignik flora may be correlative to the Sable Mountain flora.

A high diversity is thought to indicate a warm and humid climate (Golovneva and Herman, 1998). The Chignik florule as described by Hollick (1930) from six different collections made at the beginning of the 20th century between Chignik Bay and Pavlof Bay on the Alaska Peninsula in southwest Alaska includes the cycadophyte *Nilssonia serotina* Heer, a small leaf ginkgophyte, and a significant number of dicot angiosperm morphotypes including thermophilic taxa such as *Cupanites*, '*Cornus*,' and magnoliid and lauroid forms in addition to the cupressaceous conifer genera *Cephalotaxopsis*, *Sequoia*, *Metasequoia* and possible *Glyptostrobus*. The taxonomy is in need of revision. Many of Hollick's (1930) taxonomical designations represent morphological variations of a single genus and many of the familial and generic designations are invalid by the standards of current plant systematics. However, it is evident that the dicot angiosperm diversity is significantly greater than that of the Sable Mountain flora. For a comparison, we constrained 34 angiosperm morphotypes from the figured and described specimens of the Chignik florule. The largest collection, the T. W. Stanton collection from Chignik Bay, comprises 13 morphotypes; the proportion of entire leaf blades is 31%. This compares to about 10% for the Sable Mountain flora.

If the T. W. Stanton collection were to represent the full angiosperm diversity for the time of deposition, an LMA application using the regression equation of Wolfe (1979) would indicate a MAT estimate of 11° C for the florule at Chignik Bay. Additional entire-margined leaves are described by Hollick (1930) from the other five collections, and if any two or all of these are coeval with Chignik Bay specimens, the MAT estimate could rise to 13° C. More data are needed, however, to support this supposition.

It is not clear how the fossil localities compare with those of the lower Cantwell Formation. The alluvial fan interpretation for the coarser-grained non-marine facies of the Chignik Formation (Mancini et al., 1978) suggests a mountainous terrain bordering a narrow coastal plain consistent with an active plate margin. Thus, aspects of the depositional system may have been similar to that of the lower Cantwell Formation. The paleolatitudinal position of the Chignik Formation is poorly constrained from paleomagnetic analyses of the Chignik, and the more distally deposited Hoodoo and overlying late Paleocene Tolstoi formations, all of which yielded anomalously low and inconsistent paleolatitude results (Stone et al., 1982; Hillhouse and Coe, 1994). The Cretaceous paleoposition of the Alaska Peninsula remains controversial because of the difficulty in predicting the amount and timing of northward translation of outboard terranes along the Tintina and Denali fault systems during the late Cretaceous and earliest Tertiary and because of a possible 40 – 50° counterclockwise rotation of southern and southwestern Alaska during early Tertiary time (Hillhouse and Coe, 1994; Till et al., 2007b). However, a relatively high paleolatitude can be assumed from 2 well-constrained paleomagnetic sites located in relative proximity on either side of the late Mesozoic terrane boundary: Latest Cretaceous volcanic rocks on Hagemester Island (paleolatitude 65° ± 4° N) and near Lake Clark, located on the northern Peninsula Terrane ~350 km to the northeast (paleolatitude 63° ± 9° N). The similarity of the results indicates that the two sites have not moved significantly along meridional lines relative to each other within error since 66 Ma (Hillhouse and Coe, 1994). Thus, if the age of the Chignik florule is indeed coeval with the Sable Mountain florule, the apparent MAT differences may indicate a stronger

polar temperature gradient than previously thought.

Evidence for a warm climate at a relatively high latitude may be correlative with proximity to an ocean. Both the Prince Creek Formation and the Chignik Formation depositional environments may have been warmed by a maritime climate (Fiorillo, 2008; Fiorillo et al., 2010). Frakes (1999) and Zakharov et al. (1999, 2011) independently suggest a warm period during the latest Campanian. Frakes (1999) calculated sea surface temperatures between 15 and 20° C at paleolatitudes ranging from 35 to 65° N. Zakharov et al. (2011) obtained seawater temperatures of 19.4 – 25.5° C for the latest Campanian from oxygen isotope ratios of aragonitic ammonoid and inoceramid bivalve shells from the Matanuska Formation of southern Alaska. The many marine tongues of the Chignik Formation and a coal-bearing member suggest that it was deposited in a paralic setting. Thus, the high proportion of entire-margined woody dicot leaves in the Chignik flora was likely a result of warm sea surface temperatures.

By the earliest Maastrichtian, sea surface temperatures had declined to 10 to 15° C at high latitudes (Frakes, 1999; Zakharov et al., 2011) and continued to fall to 7° C at Sakhalin Island as determined by Zakharov et al. (1999) using brachiopods and ammonite carbon and oxygen isotope paleotemperature estimates. Therefore, the high diversity of the Chignik flora, including its thermophilic connotation, is more compatible with a latest Campanian age and climate optimum. Moreover, a magnoliid taxon ("*Magnolia*" *palaeauriculata* Hollick) described by Hollick (1930) from the Chignik Formation has also been identified from a basal and therefore possibly older section of the Cantwell Formation in addition to cycadophyte and ginkgophyte fossil material (Alaska Paleontological Database, 2014).

In contrast, the less thermophilic Sable Mountain floral composition was likely influenced by the cooler climate of the early Maastrichtian. The retreat of the CWIS could also have led to cooler inland temperatures reducing poleward heat transfer and increasing continentality. This could explain the larger proportion of toothed leaf margins and lower angiosperm diversity, which correlate with cooler temperatures (Wolfe, 1987; Wolfe and Spicer, 1999; Spicer and Herman, 2010). To solve the

puzzle posed by the richness of the Chignik florule, better chronostratigraphic control is required for the Chignik Formation. As long as refined age constraints are lacking, we must conclude that the two floras represent two very different phytogeographic provinces, one with a cool temperate continental flora and the other with a warm temperate maritime-influenced flora. The strong temperature gradient implied by the paleobotanical data for the southern half of ancient Alaska, however, is inconsistent with the predicted more shallow latitudinal temperature gradient for the Maastrichtian (see Spicer and Herman, 2010).

Implications for Paleoecology and Paleoenvironment

The new U–Pb zircon ages and paleolatitude assessments validate the comparisons and correlations of fossil and stratigraphic data, both intra- and extra-basinal. Age differences could be an explanation for observed differences in the floral compositions. To-date, the Sable Mountain flora comprises 42 species; the Chignik flora (as described by Hollick, 1930) comprises an estimated 50 species, yet the two megaflores have few genera in common. Shared taxa are the fern genera *Cladophlebis*, the conifer genera *Cephalotaxopsis*, *Metasequoia* and possibly *Glyptostrobus* and the angiosperm genera *Trochodendroides*, *McClintockia*, and *Celastrinites*. Conifer diversity appears to be greater in the Sable Mountain flora. Angiosperm diversity is higher in the Chignik flora; yet, it lacks long-ranging taxa, most notably menispermoids and platanoids and newer taxa such as *Corylites*. Platanoids are an important taxonomic group in the Cantwell flora, the more southerly deposited Kundur Formation (Van Itterbeeck et al., 2005; Golovneva et al., 2008), and the Koryak and Kakanaut formations (Golovneva et al., 2008; Moiseeva, 2008; Krassilov et al., 2009).

Perhaps as a result of the early Maastrichtian cooling and greater continentality including along the Beringian land bridge, hamamelidaceous and betulaceous dicot taxa and several different monocot taxa become more dominant, replacing platanoid groups. For example, *Corylites beringianus* and other betulaceous leaves, and linear (*Phragmites*- and *Typha*-like) and broad-leaved (*Potamogeton*- and *Alisma*-like) monocots appear in the lower Cantwell Formation by the earliest Maastrichtian and in the

Far North by the mid- to late Maastrichtian where they remain dominant throughout the Paleocene in the northeast Asian floras and the Danian–Selandian Sagwon flora of northern Alaska (Sagavanirktok river basin) (Golovneva, 2000b; Moiseeva, 2008; Moiseeva et al., 2009; Herman et al., 2009; Krassilov et al., 2009). The floristic data from the lower Cantwell Formation contradict the hypothesis that late Cretaceous plants radiated in, and spread from, northeastern Russia to North America. A major floral reorganization, similar to the one occurring at high latitudes at the early Maastrichtian boundary, is not observed at the K/T boundary in the Beringian realm (Herman et al., 2009; Krassilov et al., 2009) likely because the succeeding low diversity boreal flora was well-adapted to short seasons and temperature variability.

One intriguing attribute of the Sable Mountain florule and other floral assemblages of the lower Cantwell Formation (Wolfe and Wahrhaftig, 1970; Wright, unpublished data) is the co-occurrence of ferns, sphenophytes, conifers, and dicot and monocot angiosperms all evidently having grown in close proximity. Ten to possibly twelve conifer genera were reported. These are c.f. *Pityophyllum*, *Cephalotaxopsis*, *Tumion*, *Taxodium*, *Metasequoia*, possible *Parataxodium*, *Glyptostrobus*, *Sequoia*, *Larix*, *Pinus*, *Picea*, and specimens assignable to *Thuja* or *Mesocyparis*. Except for the latter, all of these occur at Sable Mountain. This great conifer diversity is similar to what Golovneva et al. (2008) and Herman et al. (2009) report from the Kundur and Taipinglinchang formations of the Amur region and might suggest similar geographic attributes. The mix of arboreal and non-arboreal taxa shows that edaphic conditions were frequently changing. This could be the result of infrequent and uneven deposition. For example, in his study on alluvial fan depositional processes, Bull (1977) writes that vegetation has an important role in alluvial fan deposition and suggests that lush low-growing vegetation could have slowed sheet flow currents resulting in rapid sediment accumulation on the alluvial fan slope. Consequently, floodplain forests remained immature, providing room for invaders.

Unlike the Sable Mountain flora, the Chignik flora does not appear to contain relict angiosperm genera. Possibly, the Arctic provided niches for

early late Cretaceous taxa that had gradually migrated north. For example, very large leaves of *Pseudoprotophyllum* and *Menispermites* were recovered from the base to mid-section at Sable Mountain in deposits that we interpret to be of late Campanian age. Higher in our section, in inferred Maastrichtian strata, leaf size is notably reduced for both taxa. Hollick (1930) described several specimens of *Pseudoprotophyllum* from the Cenomanian (and Turonian?) Melozi Formation of the Yukon River Valley in west-central Alaska that are now considered to be synonyms of *Pseudoprotophyllum boreale* (Dawson) Hollick, emend. Golovneva (Golovneva, 2009) and include very large leaf forms. *Pseudoprotophyllum boreale* (or synonyms) were described from Cenomanian to Coniacian fossil localities throughout northern and northeastern Asia, the North Slope of Alaska, and Northwestern Canada (Hollick, 1930; Herman, 2007; Golovneva, 2009), indicating it was widely distributed at a time when platanoid groups were highly diversified (Golovneva, 2009). *Pseudoprotophyllum* is apparently absent from the Maastrichtian Kakanaut and Koryak floras and the Chignik flora, but has been observed in a concretion from Paleocene strata on the North Slope of Alaska (Peter Flaig and Dolores van der Kolk, pers. comm.) and in early Tertiary beds of Axel Heiberg Island in the Canadian Arctic Archipelago (McIver and Basinger, 1999). The fact that such long-ranging species or relict species occur in the Cantwell Formation and in the High Arctic during the early Tertiary indicates that inland basins like the Cantwell basin could have served as temporary refugia during the warm stage of the late Campanian.

Leaves of non-woody angiosperms are rarely preserved in the megafloral record because they wilt on the plant and wither. Evidence for the presence of herbaceous plants therefore comes from pollen records. A relatively diverse angiosperm pollen flora recorded from the Prince Creek Formation (Frederiksen, 1991; Brandlen, 2008; Flaig et al., 2013) is poorly matched by the plant megafossil record (Spicer and Parrish, 1990a; Spicer and Herman, 2010). As a consequence, Spicer and Herman (2010) suggested the presence of herbaceous plants which would have left no foliar record. Additional evidence for herbaceous plant growth comes from root casts. Perennial root structures (rhizomes, bulbs, tubers;

Fig. 9), from which new shoots grow, allow plants to reproduce asexually. Their ability to store nutrients, food, and water and enter dormancy protects them against drought, lack of nutrients, a short growing season, and foraging (Shewry, 2003; Bell, 2008; Gómez-García et al., 2009). This provides for more regulated growth and a competitive advantage in places where adverse growing conditions prevail (Gómez-García et al., 2009). Botanical evidence seems to suggest that perennating plants are more successful at colonizing environmental niches marked by extremes (Geneve, 2006).

Tubers form by thickening along a portion of a root. Although apparently rare and probably of little taxonomic value, we report on two specimens resembling casts of tubers (Fig. 9) that indicate that some, possibly herbaceous plants entered dormancy at the onset of the low-level light season or a drought period. The significance of the find is appreciated, because it suggests that a) grounds were basically frost-free, b) growing conditions were periodically unfavorable for some plants, and c) the tubers could have provided food for ground-dwelling mammals and possibly for herbivorous dinosaurs. Selection for asexual reproduction may have been an adaptive response to short growing seasons and periodically adverse growing conditions.

As with the paleobotanical data, helpful taxonomic information for vertebrate track-makers can be learned from coeval fossil-bearing beds of other high-latitude localities. In southern Alaska, an ankylosaur skull was excavated from Campanian–Maastrichtian? Matanuska Formation (Gangloff, 1995; Fiorillo, 2006). In northern Alaska, the teeth, bones, and several skulls of small and large theropods, troodontids (e.g., *Troodon formosus*; Fiorillo and Gangloff, 2000; Fiorillo et al., 2009b), hypsilophodontids, dromaeosaurids, ornithomimids, ceratopsids (e.g., *Pachyrhinosaurus perotorum*) and hadrosaurids (e.g., *Edmontosaurus*) have been excavated from the world-renowned early Maastrichtian bonebeds of the Prince Creek Formation along the Colville River on the North Slope (Rich et al., 2002; Fiorillo, 2006; Fiorillo et al., 2009b; Fiorillo et al., 2010; Gangloff and Fiorillo, 2010).

From northeastern Russia, Godefroit et al. (2009) report on a highly diverse fossil bone fauna

from a late Maastrichtian section of the Kakanaut Formation. These authors list teeth and fragmentary bone remains that can be tentatively identified to basal ornithopods, theropods, troodontids (including *Troodon cf. formosus*), dromaeosaurids, ceratopsids (ankylosaurs) and hadrosaurids. The close taxonomic association with the fauna of the Prince Creek Formation suggests similar food sources and supports the hypothesized bidirectional exchange along a surmised continental bridge (Fiorillo, 2008; Godefroit et al., 2009). The argument that dinosaurs resided year-round is strengthened by abundant skeletal remains of juvenile hadrosaurs and egg shell fragments (Golovneva, 2000a; Clemens and Nelms, 1993; Godefroit et al., 2009; Gangloff and Fiorillo, 2010; Fiorillo et al., 2010) in combination with *Edmontosaurus* bone histology data (Chinsamy et al., 2012). Krassilov et al. (2009) suggest that herbivorous dinosaurs fed on non-deciduous freshwater plants. The latest Campanian and Maastrichtian megafloral record of Eurasia and North America contains diverse monocots and dicot angiosperms that are thought to have formed aquatic communities. Their adaptive radiation occurred seemingly parallel in the northern hemisphere and, in a mutual dependence, may have corresponded closely with the expansion of dinosaurs into the boreal realm (Krassilov et al., 2009).

CONCLUSIONS

New numerical ages of 71.5 ± 0.9 Ma and 71.0 ± 1.1 Ma for the non-marine lower Cantwell Formation at Sable Mountain in Denali National Park, Alaska, establish a concise temporal framework for the Sable Mountain deposits, provide stratigraphic control, and enable valid biostratigraphic and geographic correlations. The new ages place dinosaur, pterosaur and bird footprints, and the Sable Mountain florule into the late Campanian and earliest Maastrichtian and approximate the boundary between these two important epochs. Early Maastrichtian lower Cantwell strata at Sable Mountain are the same age as the dinosaur bone-bearing beds of the Prince Creek Formation on the North Slope of Alaska which may serve as an analogue for ecological reconstructions of the lower Cantwell Formation. Dating of the bird ichnotaxa provides correlation with both Northern Asian and North American faunas supporting the

concept of a Panberingian land connection during a period of global warmth. The Sable Mountain section may also be correlative to the Chignik Formation of southwestern Alaska; however, the latter bears a warm temperate flora while the Sable Mountain flora is characterized as a cool temperate flora, suggesting that the two floras represent different phytogeographic provinces located in relative proximity. The Cantwell flora is characteristic of the polar broad-leaved deciduous forest that was widely distributed across the Arctic in the Late Cretaceous and early Tertiary and was highly adapted to withstand adverse conditions. Several taxonomic groups resemble those described from the mid to late Maastrichtian Koryak flora of the Othotsk-Chukotka volcanogenic belt in northeastern Russia. The fluvial valleys that supported these two floras were similarly surrounded by dissected uplands. The late Campanian to early Maastrichtian age for the Cantwell strata negates the idea put forward by previous workers that the Koryak flora radiated and expanded from Russia to the North Slope of Alaska. The morphological similarities between the Asian and North American taxa support the supposition of floristic and faunal exchanges across the Beringian landbridge, but the timing remains poorly constrained. We argue that the diversity and structure of different phytogeographic regions is closely linked to the migration of faunal groups in a mutual dependence and to local environmental and geographic factors.

Age relationships between outcrops at Sable Mountain, Polychrome Mountain and Double Mountain in Denali National Park and Preserve reveal that complexly distributed lithofacies are correlative at least in part and are the result of point-sourcing and local controls on deposition related to an alluvial fan depositional system and adjacent environments. Debris flows, rapid basin center subsidence, and a high sediment supply from synchronously uplifted basin margins are consistent with an inferred location in an orogenic belt.

ACKNOWLEDGMENTS

This research was generously funded by BP, the Alaska Geological Society and the National Park Service. We also thank the Denali National Park Administration, especially Paul Anderson, Philip

Hooge, Lucy Tyrrell, Linda Stromquist, Denny Capps, and the late Phil Brease for supporting this research and for much appreciated logistical support. Bernie Housen of the University of Western Washington and his graduate students are thanked for analyzing and measuring magnetic vectors on our paleomagnetic sample. Furthermore, we thank Anne Pasch for her time and willingness to review this manuscript and much appreciate her comments. Sarah Fowell is acknowledged for her time in the field and her professional advice. Equally so, we are much indebted to field assistants Eric Brandlen, Ephy Wheeler, Anja Kircher, Todd Jacobus, Joshua Payne, Colby Wright and Anna Liljedahl, and to Maciej Slivinski for help in the laboratory.

REFERENCES

- Alaska Paleontological Database, 2014. [<http://www.alaskafossil.org>] Last accessed January 24, 2014.
- Bacon, C.R., Foster, H.L., and Smith, J.G., 1990. Rhyolitic Calderas of the Yukon-Tanana Terrane, East-central Alaska: Volcanic Remnants of a Mid-Cretaceous Magmatic Arc. *Journal of Geophysical Research* 95, B13, 21-451–21-461.
- Bell, A.D., 2008. *Plant Forms: An Illustrated Guide to Flowering Plant Morphology*. Timber Press Portland–London, 432 p.
- Bell, W.A., 1949. Uppermost Cretaceous and Paleocene floras of western Alberta. *Geological Survey of Canada Bulletin* 13, 231 p.
- Benowitz, J.A., Layer, P.J., Armstrong, P., Perry, S.E., Haeussler, P.J., Fitzgerald P.G., and VanLaningham, S., 2011. Spatial variations in focused exhumation along a continental-scale strike-slip fault: The Denali Fault of the eastern Alaska Range. *Geosphere* 7 (3), 455–467, DOI: 10.1130/GES00589.1.
- Benowitz, J.A., Haeussler, P.J., Layer, P.W., O’Sullivan, P.B., Wallace, W.K., and Gillis, R.J., 2012. Cenozoic tectono-thermal history of the Tordrillo Mountains, Alaska: Paleocene–Eocene ridge subduction, decreasing relief, and late Neogene faulting. *Geochemistry, Geophysics, Geosystems*, 13, Q04009, DOI: 10.1029/2011GC003951.
- Benowitz, J.A., Haeussler, P.J., Layer, P.W., O’Sullivan, P.B., Wallace, W.K., and Gillis, R.J., 2012. Cenozoic tectono-thermal history of the Tordrillo Mountains, Alaska: Paleocene–Eocene ridge subduction, decreasing relief, and late Neogene faulting. *Geochemistry, Geophysics, Geosystems*, 13, Q04009, DOI: 10.1029/2011GC003951.
- Billingsley, R.L. 1977. The Cantwell Formation (Paleocene) as a possible offset feature along the Denali Fault, central Alaska Range, Alaska. [M.S. Thesis], University of Wisconsin, Madison, Wisconsin, 86 p.
- Blair T. C. and McPherson, J.G., 1994. Alluvial fans and their natural distinction from rivers based on morphology, hydraulic processes, sedimentary

- processes, and facies assemblages. *Sedimentary Geology* A64 (3), 450–489.
- Bradley, D.C., Kusky, T.M., Haeussler, P.J., Rowley, D.C., Goldfarb, R.J., and Nelson, S.W., 2003. Geologic signature of early Tertiary ridge subduction in the accretionary wedge, forearc basin, and magmatic arc of south-central Alaska. In: Sisson, V.B., Roeske, S., and Pavlis, T.L. (eds.) *Geology of a Transpressional Orogen Developed during a Ridge–Trench Interaction along the North Pacific Margin*. Geological Society of America Special Paper 371, 19–50.
- Braman, D.R. and Sweet, A.R., 2012. Biostratigraphically useful Late Cretaceous–Paleocene Terrestrial palynomorphs from the Canadian Western Interior Sedimentary Basin. *Palynology* 36 (1), 8–35. DOI:10.1080/01916122.2011.642127.
- Brandlen, E., 2008. Paleoenvironmental reconstruction of the Late Cretaceous (Maastrichtian) Prince Creek Formation, near the Kikak Tegoseak dinosaur quarry, North Slope, Alaska. [Unpublished M.S. Thesis], University of Alaska Fairbanks, Fairbanks, Alaska, 225 p.
- Bull, W.B., 1977. The alluvial fan environment. *Progress in Physical Geography* 1, pp. 222–270.
- Capps, S.R., 1919. The Kantishna Region, Alaska. *United States Geologic Survey Bulletin* 687, 30–45.
- Capps, S.R., 1940. The Geology of the Alaska Railroad region. *United States Geologic Survey Bulletin* 907, 201 p.
- Chinsamy, A., Thomas, D.B., Tumarkin-Deratzian, A.R., and Fiorillo, A.R., 2012. Hadrosaurs were perennial polar residents. *The Anatomical Record* 295, 610–614.
- Chew, D.M. and Donelick, R.A., 2012. Combined apatite fission track and U–Pb dating by LA–ICP–MS and its application in apatite provenance analysis. In: Sylvester, P., *Quantitative Mineralogy and Microanalysis of Sediments and Sedimentary Rocks*. Mineralogical Association of Canada Short Course 42, St. John's, Newfoundland and Labrador, 219–247.
- Clemens, W.A., 1994. Continental vertebrates from the Late Cretaceous of the North Slope, Alaska. In: Thurston, D. K. and Fujita, K. (eds.) 1992 *International Conference on Arctic Margins, Proceedings*. United States Department of Interior Mineral Management Service, Outer Continental Shelf Study MMS 94-0040, pp. 395–398.
- Clemens, W.A. and Nelms, L.G., 1993. Paleocological implications of Alaskan terrestrial vertebrate fauna in latest Cretaceous time at high paleolatitudes. *Geology* 21, 503–506.
- Cole, R.B., Ridgway, K.D., Layer, P.W., and Drake, J., 1999. Kinematics of basin development during the transition from terrane accretion to strike-slip tectonics, Late Cretaceous-early Tertiary Cantwell Formation, south-central Alaska. *Tectonics* 18 (6), 1224–1244, DOI: 10.1029/1999TC900033.
- Cole, R.B., Nelson, S.W., Layer, P.W., and Oswald, P.J., 2006. Eocene volcanism above a depleted slab window in southern Alaska. *Geological Society of America Bulletin* 118 (1/2), 140–158, DOI: 10.1130/B25658.1.
- Cole, R.B., Layer, P.W., Hooks, B., Cyr, A., and Turner, J., 2007. Magmatism and deformation in a terrane suture zone south of the Denali Fault, northern Talkeetna Mountains, Alaska. In: Ridgway, K.D., Trop, J.M., Glen, J.M., and O'Neil, J.M. (eds.) *Tectonic Growth of a Collisional Continental Margin: Crustal Evolution of Southern Alaska*. Geological Society of America Special Paper 431, 447–506, DOI: 10.1130/2007.2431(19).
- Conrad, J.E., McKee, E.H., and Turrin, B.D., 1992. Age of Tephra Beds at the Ocean Point Dinosaur Locality, North Slope, Alaska, based on K–Ar and $^{40}\text{Ar}/^{39}\text{Ar}$ analyses. *United States Geological Survey Bulletin* 1990-C, C1–C12.
- Corfu, F., 2013. A century of U–Pb geochronology: The long quest towards concordance. *Geological Society of America Bulletin* 125 (1–2), 33–47, DOI: 10.1130/B30698.1.
- Csejtey, B., Mullen, M.W., Cox, D.P., and Stricker, G.D., 1992. Geology and geochronology of the Healy quadrangle, south-central Alaska. *United States Geological Survey Miscellaneous Investigation Series I-1961*, 63 p., 2 plates, scale 1:250,000.

- Detterman, R.L., Case, J.E., Miller, J.W., Wilson, F.H., Yount, M.E., 1996. Stratigraphic framework of the Alaska Peninsula. *United States Geological Survey Bulletin* 1969-A, 1–74.
- Dickinson, W.R., Beard, L.S., Brackenridge, G.R., Erjavec, J.L., Ferguson, R.C., Inman, K.F., Knepp, R.A., Lindberg, F.A., and Ryberg, P.T., 1983. Provenance of North American Phanerozoic sandstones in relation to tectonic setting. *Geological Society of America Bulletin* 94 (2), 222–235.
- Donelick, R.A., O’Sullivan, P.B., and Donelick, M.B., 2010. A Discordia-Based Method of Zircon U-Pb Dating from LA-ICP-MS Analysis of Single Spots. *Smart Science for Exploration and Mining*, v. 1 and 2, p. 276–278.
- Eldridge, G.H., 1900. A reconnaissance in the Sushitna Basin and adjacent territory, Alaska, in 1898. *United States Geological Survey 20th Ann. Report*, part 7, 1–29.
- Falcon-Lang, H.J., McRhae, R.A., and Czank, A.Z., 2004. Palaeoecology of Late Cretaceous polar vegetation preserved in the Hansen Point Volcanics, NW Ellesmere Island, Canada. *Palaeogeography. Palaeoclimatology. Palaeoecology* 212 (3), 45–64.
- Fiorillo, A.R., 2004. The dinosaurs of Arctic Alaska. *Scientific American* 291 (6), 84–91.
- Fiorillo, A.R., 2006. Review of the dinosaur record of Alaska with comments regarding Korean dinosaurs as comparable high-latitude fossil faunas. *Journal of Paleontological Society of Korea* 22 (1), 15–27.
- Fiorillo, A.R., 2008. Cretaceous dinosaurs of Alaska: Implications for the origins of Beringia. In: Blodgett, R.B., and Stanley, G. (eds.) *The Terrane Puzzle: new perspectives on paleontology and stratigraphy from the North American Cordillera*. Geological Society of America Special Paper 442, 313–326, DOI: 10.1130/2008.442(15).
- Fiorillo, A.R., and Gangloff, R.A., 2000. Theropod teeth from the Prince Creek Formation (Cretaceous of Northern Alaska, with speculations on Arctic Dinosaur paleoecology. *Journal of Vertebrate Paleontology* 20 (4), 675–682.
- Fiorillo, A.R. and Gangloff, R.A., 2001. The caribou migration model for Arctic hadrosaurs (Ornithischia: Dinosauria): a reassessment. *Historical Biology* 15, 323–334.
- Fiorillo, A.R. and Parrish, J.T., 2004. The first record of a dinosaur from southwestern Alaska. *Cretaceous Research* 25, 453–458.
- Fiorillo, A.R. and Adams, T., 2012. A therizinosaur track from the lower Cantwell Formation (Upper Cretaceous) of Denali National Park, Alaska. *Palaios* 27, 395–400, DOI: 10.2110/palo.2011.p11-083r.
- Fiorillo, A.R. and Tykoski, R.S., 2012. A new species of the centrosaurine ceratopsid *Pachyrhinosaurus* from the North Slope (Prince Creek Formation: Maastrichtian) of Alaska. *Acta Palaeontologica Polonica* 57 (3), 561–573.
- Fiorillo, A.R., McCarthy, P.J., Breithaupt, B.H., and Brease, P.F., 2007. Dinosauria and fossil aves footprints from the lower Cantwell Formation (Latest Cretaceous), Denali National Park and Preserve. *Alaska Park Science* 6, 41–43.
- Fiorillo, A.R., Hasiotis, S.T., Kobayashi, Y. and Tomsich, C.S., 2009a. A pterosaur manus track from Denali National Park, Alaska Range, Alaska, United States. *Palaios* 24, 466–472, DOI: 10.2110/palo.2008.p08-129r.
- Fiorillo, A.R., Tykoski, R.S., Currie, P.J., McCarthy, P.J., and Flaig, P., 2009b. Description of Two Partial *Troodon* Braincases from the Prince Creek Formation (Upper Cretaceous), North Slope Alaska. *Journal of Vertebrate Paleontology* 29, 178–187.
- Fiorillo, A.R., McCarthy, P.J., and Flaig, P.P., 2010. Taphonomic and sedimentologic interpretations of the dinosaur-bearing upper Cretaceous strata of the Prince Creek formation, Northern Alaska: Insights from an ancient high-latitude terrestrial ecosystem. *Palaeogeography. Palaeoclimatology. Palaeoecology* 295 (3), 376–388, DOI: 10.1016/j.palaeo.2010.02.029.
- Fiorillo, A.R., Hasiotis, S.T., Breithaupt, B.H., Kobayashi, Y., and McCarthy, P.J., 2011. Bird tracks from the Upper Cretaceous Cantwell Formation of Denali National Park, Alaska, USA: a new perspective on ancient northern polar vertebrate biodiversity. *Journal of Systematic Paleontology* 9 (1), 33–49, DOI: 10.1080/14772019.2010.509356.

- Fiorillo A.R., Contessi, M., Kobayashi, Y., and McCarthy, P.J., 2014. Theropod tracks from the lower Cantwell Formation (Upper Cretaceous) of Denali National Park, Alaska, USA with comments on theropod diversity in an ancient, high-latitude terrestrial ecosystem. In: Lockley, M. and Lucas, S.G. (eds.) *Tracking Dinosaurs and other tetrapods in North America*. New Mexico Museum of Natural History and Science, pp. 429-439.
- Flaig, P.P., 2010. Depositional environments of the Late Cretaceous (Maastrichtian) dinosaur-bearing Prince Creek Formation: Colville River region, North Slope, Alaska. [Unpublished Ph.D. Dissertation], University of Alaska Fairbanks, Fairbanks, Alaska, 311 p.
- Flaig, P.P., McCarthy, P.J., and Fiorillo, A.R., 2013. Anatomy, evolution and paleoenvironmental interpretation of an ancient Arctic coastal plain: Integrated paleopedology and palynology from the Upper Cretaceous (Maastrichtian) Prince Creek Formation, North Slope, Alaska, USA. In: Driese, S.G. and Nordt, L.C. (eds) *New Frontiers in Paleopedology and Terrestrial Paleoclimatology*. SEPM Special Publication 104, 179–230.
- Foster, H.L. and Igarashi, Y., 1990. Fossil pollen from non-marine sedimentary rocks of the eastern Yukon-Tanana region, east-central Alaska. In: Dover, J.H. and Galloway, J.P. (eds.) *Geologic Studies in Alaska by the United States Geological Survey in 1989*. United States Geological Survey Bulletin 1946, 11–20.
- Foster, H.L., Keith, T.E.C., and Menzie, W.D., 1994. The geology of the Yukon Tanana area of east-central Alaska. In: Plafker, G. and Berg, H.C. (eds.) *The Geology of Alaska*. Boulder, Colorado, Geological Society of America. *The Geology of North America*, Vol. G-1, pp. 205–214.
- Frakes, L.A., 1999. Estimating global thermal state from Cretaceous sea surface and continental temperature data. In: Barrera, E. and Johnson, C.C. (eds.) *Evolution of the Cretaceous Ocean–Climate System*. Geological Society of America Special Paper 332, 49–57.
- Frederiksen, N.O., 1991. Pollen zonation and correlation of Maastrichtian marine beds and associated strata, Ocean Point dinosaur locality, North Slope, Alaska. United States Geological Survey Bulletin 1990-E, E1–E24, 7 plates.
- Gangloff, R.A., 1995. *Edmontonia* sp., the first record of an ankylosaur from Alaska. *Vertebrate Paleontology* 15 (1), 195–200.
- Gangloff, R.A. and Fiorillo, A.R., 2010. Taphonomy and paleoecology of a bonebed from the Prince Creek Formation. *Palaios* 25, 299–317.
- Geneve, R.L., 2006. Alternative strategies for clonal plant reproduction. *Combined Proceedings International Plant Propagators' Society* 56, pp. 269-273.
- Gilbert, W.G. and Redman, E., 1975. Geologic map and structure sections of Healy C-6 Quadrangle, Alaska: Alaska Division of Geological and Geophysical Surveys Open-File Report 80, 1 sheet, scale 1:40,000.
- Gilbert, W.G., Ferrell, V.M., and Turner, D.L., 1976. The Teklanika Formation—A new Paleocene volcanic formation in the central Alaska Range. Alaska Division of Geological and Geophysical Surveys Geologic Report 47, 16 p.
- Godefroit, P., Golovneva, L., Shczepetov, S., Garcia, G., and Alekseev, P., 2009. The last polar dinosaurs: High diversity of latest Cretaceous arctic dinosaurs in Russia. *Naturwissenschaften* 96, 495–501.
- Golovneva, L.B., 1994. The flora of the Maastrichtian-Danian deposits of the Koryak Uplands, Northeast Russia. *Cretaceous Research* 15 (1), 89–100.
- Golovneva, L.B., 2000a. Maastrichtian Climate in the Northern Hemisphere. *Geological Society of London Special Publication* 181, 43–54.
- Golovneva, L.B., 2000b. Aquatic plant communities at the Cretaceous-Palaeogene boundary in northeastern Russia. *Acta Paleobotanica* 42 (2), 139–151.
- Golovneva, L.B., 2009. The Morphology, Taxonomy, and Occurrence of the Genus *Pseudoprotophyllum* Hollick (Platanaceae) in Late Cretaceous Floras of Northern Asia. *Paleontological Journal* 43 (10), 1230–1244.
- Golovneva, L.B. and Herman, A.B., 1998. Regularities in the Late Cretaceous flora evolution. *Stratigraphy and Geological*

- Correlation 6 (6), 537–549.
- Golovneva, L. B., Sun, G., and Bugdaeva, E. V., 2008. Campanian Flora of the Bureya River Basin (Late Cretaceous of the Amur River region). *Paleontological Journal* 42 (5), 554–567.
- Gómez-García, D., Azorín, J., and Aguirre, A.J., 2009. Effects of small-scale disturbances and elevation on the morphology, phenology and reproduction of a successful geophyte. *Journal of Plant Ecology* 2 (1), 13–20, DOI: 10.1093/jpe/rtp003.
- Hampton, B.A., Ridgway, K.D., O’Neill, J.M., Gehrels, G.E., Schmidt, J., and Blodgett, R.B., 2007. Pre-, syn-, and post-collisional stratigraphic framework and provenance of Upper Triassic–Upper Cretaceous strata in the northwestern Talkeetna Mountains, Alaska. In: Ridgway, K.D., Trop, J.M., Glen, J.M., and O’Neil, J.M. (eds.) *Tectonic Growth of a Collisional Continental Margin: Crustal Evolution of Southern Alaska*. Geological Society of America Special Paper 431, 401–438, DOI: 10.1130/2007.2431(16).
- Hampton, B.A., Ridgway, K.D., and Gehrels, G.E., 2010. A detrital record of Mesozoic island arc accretion and exhumation in the North American Cordillera: U–Pb geochronology of the Kahiltna basin, southern Alaska. *Tectonics* 29 TC 4015, 1–21, DOI: 10.1029/2009TC002544.
- Harris, J.D., Johnson, K.R., Hicks, J., and Tauxe, L., 1996. Four-toed theropod footprints and a paleomagnetic age from the Whetstone Falls Member of the Harebell Formation (Upper Cretaceous: Maastrichtian), northwestern Wyoming. *Cretaceous Research* 17, 381–401.
- Hasiotis, S. T., 2002. Continental Trace Fossils. *SEPM Short Course Notes* 51, 132 p.
- Hasiotis, S.T., Fiorillo, A.R., Kobayashi, Y., and Brease, P., 2009. Preliminary report on the microbial, invertebrate, and vertebrate trace fossils from Denali National Park and Preserve, Alaska: Insights into the biodiversity of a polar ecosystem. *Geological Society of America Abstracts with Programs* 41 (7), p. 162.
- Hasiotis, S.T., Fiorillo, A.R., and Kobayashi, Y., 2011. Invertebrate and vertebrate ichnofossils from the lower part of the Upper Cretaceous Cantwell Formation, Denali National Park, Alaska: Insights into the paleoenvironments, paleo-hydrology and paleoclimate of high-latitude continental paleoecosystems: AAPG Pacific Section Program with Abstracts, Anchorage Alaska, May 6–14, 2011, p. 60.
- Hay, W.W., 2008. Evolving ideas about the Cretaceous climate and ocean circulation. *Cretaceous Research* 29, 725–753, DOI: 10.1016/j.cretres.2008.05.025.
- Herman, A.B., 2007. Comparative Paleofloristics of the Albian–Early Paleocene in the Anadyr–Koryak and North Alaska Subregions. Part 3: Comparison of Floras and Floristic Changes across the Cretaceous–Paleogene Boundary. *Stratigraphy and Geological Correlation* 150 (5), 512–524.
- Herman, A.B. and Spicer, R.A., 1995. Latest Cretaceous Flora of Northeastern Russia and the Terminal Cretaceous Event. *Paleontological Journal* 29 (2), 22–35.
- Herman, A.B., Akhmetiev, M.A., Kodrul, M., Moiseeva, M.G., and Iakovleva, A.I., 2009. Flora Development in Northeastern Asia and Northern Alaska during the Cretaceous–Paleogene Transitional Epoch. *Stratigraphic and Geological Correlation* 17 (1), 79–97.
- Hickman, R.G., 1974. Structural geology and stratigraphy along a segment of the Denali Fault system, central Alaska Range, Alaska. [Ph.D. Dissertation], University of Wisconsin, Madison, 276 p., scale 1:63,360.
- Hickman, R.G. and Craddock C., 1976. Geologic map of the central Healy Quadrangle, Alaska. Alaska Division of Geological and Geophysical Survey Open–File Report AOF-95: 1 p.
- Hickman, R.G., Sherwood, K.W. and Craddock C., 1990. Structural evolution of the early Tertiary Cantwell basin, south-central Alaska. *Tectonics* 9 (6), 1433–1449.
- Hillhouse J.W. and Gromme, C.S., 1982. Limits to northward drift of the Paleocene Cantwell Formation, central Alaska. *Geology* 10, 552–556.
- Hillhouse, J.W. and Coe, R.S., 1994. Paleomagnetic data from Alaska. In: Plafker, G., and Berg, H.C., (eds.) *The Geology of Alaska*. Boulder, Colorado, Geological Society of America. *The Geology of North America Vol. G-1*, pp. 797–812.

- Hollick, A., 1930. The upper Cretaceous floras of Alaska. United States Geological Survey Professional Paper 159, 123 p., 86 plates.
- Hoskin, P.W.O. and Schaltegger, U., 2003. The composition of zircon and igneous and metamorphic petrogenesis. *Zircon* 53, 27–62.
- Imlay R.W. and Reeside, J.B., 1954. Correlations of the Cretaceous formations of Greenland and Alaska: Geological Society of America Bulletin 65, 223–246.
- Jackson, S.J., Whyte, M.A., and Romano, M., 2009. Laboratory-controlled simulations of dinosaur footprints in sand: A key to understanding vertebrate track formation and preservation. *Palaios* 24, 222–238, DOI: 10.2110/palo.2007.p07-070r.
- Jones, D.L., Silberling, N.J., and Coney, P.J., 1983. Tectonostratigraphic and interpretive bedrock geologic map of the Mount McKinley region, Alaska. United States Geological Survey Open-File Report 83–11, scale 1:250,000.
- Kent, D.V. and Irving, E., 2010. Influence of inclination error in sedimentary rocks on the Triassic and Jurassic apparent pole wander path for North America and implications for cordilleran tectonics. *Journal of Geophysical Research* 115, B10103, 1–25, DOI: 10.1029/2009JB007205.
- Krassilov, V.A., Kodrul, T.M., and Maslova, N.P., 2009. Plant systematics and differentiation of species over trans-Beringian land connections including a newly recognized cupressaceous conifer *Ditaxocladus* Guo & Sun. *Bulletin of Geosciences* 85 (1), 95–110.
- Kumar, R., Suresh, N., Sangode, S.J., and Kumaravel, V., 2007. Evolution of the Quaternary alluvial fan system in the Himalayan foreland basin: Implications for tectonic and climatic decoupling. *Quaternary International* 159, 6–20, DOI: 10.1016/j.quaint.2006.08.010.
- Lerbekmo, J.F. and Braman, D.R., 2005. Magnetostratigraphic and palynostratigraphic correlation of late Campanian to early Maastrichtian strata of the Bearpaw and Horseshoe Canyon formations between the CPOG Strathmore corehole and the Red Deer Valley section, Alberta, Canada. *Bulletin of Canadian Petroleum Geology* 53 (2), 154–164.
- Ludwig, K.R., 2003. User's manual for Isoplot 3.00—A geochronological toolkit for Microsoft Excel. Berkeley Geochronology Center Special Publication 4, 71 p.
- Mancini, E.A. Deeter, T.M., and Wingate, F.H., 1978. Upper Cretaceous arc–trench gap sedimentation on the Alaska Peninsula. *Geology* 6, 437–439.
- Markwick, P.J. and Valdes, P.J., 2004. Palaeo-digital elevation models for use as boundary conditions in coupled ocean–atmosphere GCM experiments: A Maastrichtian (late Cretaceous) example. *Palaeogeography, Palaeoclimatology, Palaeoecology* 213, 37–63, DOI: 10.1016/j.palaeo.2004.06.015.
- McIver and Basinger, 1999. Early Tertiary floral evolution in the Canadian High Arctic. *Annals of the Missouri Botanical Garden* 86 (2), 523–545.
- Miall, A.D., 2006. *The Geology of Fluvial Deposits: Sedimentary Facies, Basin Analysis and Petroleum Geology*. Springer Verlag Berlin, 389 p.
- Moiseeva, M.G., 2008. New angiosperms from the Maastrichtian of the Amaam Lagoon area, Northeastern Russia. *Paleontological Journal* 42 (3), 313–327.
- Moiseeva, M.G., Herman, A.B., and Spicer, R.A., 2009. Late Paleocene Flora of the Northern Alaska Peninsula: The Role of Transberingian Plant Migrations and Climatic Change. *Paleontological Journal* 43 (10), 1298–1308.
- Moll-Stalcup, E.J., 1994. Latest Cretaceous and Cenozoic magmatism in mainland Alaska. In: Plafker, G., and Berg, H.C. (eds.) *The Geology of Alaska*. Boulder, Colorado, Geological Society of America. *The Geology of North America*, Vol. G-1, pp. 589–619.
- Nokleberg, W.J. and Richter, D.H., 2007. Origin of narrow terranes and adjacent major terranes occurring along the Denali Fault and in the eastern and central Alaska Range, Alaska. In: Ridgway, K.D., Trop, J.M., Glen, J.M.G., and O'Neill, J.M. (eds.) *Growth of a collisional continental margin: Crustal evolution of southern Alaska*. Geological Society of America Special Paper 431, 129–154, DOI: 10.1130/2007.2431(06).
- Nokleberg, W.J., Jones, D.L., and Silberling, N.J.,

1985. Origin and tectonic evolution of the Maclaren and Wrangellia terranes, eastern Alaska Range, Alaska. *Geologic Society of America Bulletin* 96, 1251–1270, DOI: 10.1130/0016-7606(1985)96<1251:OATEOT>2.0.CO;2.
- Nokleberg, W.J., Plafker, G. and Wilson, F.H., 1994. Geology of south-central Alaska. In: Plafker, G., and Berg, H.C. (eds.) *The Geology of Alaska*. Boulder, Colorado, Geological Society of America. *The Geology of North America*, Vol. G-1, pp. 311–366.
- Otto-Bliesner, B.L. and Upchurch, G.R., Jr., 1997. Vegetation-induced warming of high latitudes during the latest Cretaceous. *Nature* 385, 804–807.
- Palaeosens Project Members, 2012. Making sense of palaeoclimate sensitivity. *Nature* 491, 683–691, DOI: 10.1038/nature11574.
- Panuska, B.C. and D.B. Stone, 1981. Late Palaeozoic palaeomagnetic data for Wrangellia: Resolution of the polarity ambiguity. *Nature* 293, 561–563.
- Parrish, J.M., Parrish, J.T., Hutchison, J.H., and Spicer, R.A., 1987. Late Cretaceous vertebrate fossils from the North Slope of Alaska and implications for dinosaur ecology. *Palaios* 2, 377–389.
- Parrish, J.T. and Spicer, R.A., 1988. Late Cretaceous terrestrial vegetation: A near-polar temperature curve. *Geology* 16, 22–25.
- Patton, W.W., Jr., Box, S.E., and Moll-Stalcup, E.J., 1994. Geology of west-central Alaska. In: Plafker, G., and Berg, H.C., (eds.) *The Geology of Alaska*. Boulder, Colorado, Geological Society of America. *The Geology of North America*, Vol. G-1, pp. 241–269.
- Plafker, G., and Berg, H.C., 1994. Overview of the geology and tectonic evolution of Alaska. In: Plafker, G., and Berg, H.C., (eds.) *The Geology of Alaska*. Boulder, Colorado, Geological Society of America. *The Geology of North America*, Vol. G-1, pp. 989–1017.
- Pogue, J., 1915. The Cantwell Formation: A continental deposit of Tertiary age in the Alaska Range. *Journal of Geology* 23 (2), 118–128.
- Rich, T.H., Gangloff, R.A., and Hammer, W.R., 1997. Polar dinosaurs. In: Currie, P.J. and Padian, K. (eds.) *Encyclopedia of Dinosaurs*. Academic Press, San Diego, CA, 562–572.
- Rich, T.H., Vickers-Rich, P., and Gangloff, R.A., 2002. Polar dinosaurs. *Science* 295, 979–980.
- Ridgway, K.D., Trop, J.M. and Sweet, A.R., 1997. Thrust-top basin formation along a suture zone, Cantwell basin, Alaska Range: Implications for the development of the Denali Fault system. *Geological Society of America Bulletin* 109 (5), 505–523, DOI: 10.1130/0016-7606(1997)109<0505:TTB-FAA>2.3.CO;2.
- Ridgway, K.D., Trop, J.M., Nokleberg, W.J., Davidson, C.M., and Eastham, K.R., 2002. Mesozoic and Cenozoic tectonics of the eastern and central Alaska Range: Progressive basin development and deformation in a suture zone. *Geological Society of America Bulletin* 114 (12), 1480–1504, DOI: 10.1130/0016-7606(2002)114<1480:MACTOT>2.0.CO;2.
- Salazar-Jaramillo, S., McCarthy, P.J., Fowell, S.J., Benowitz, J.A., and Slivinski, M., in preparation. Sedimentology, terrestrial carbon isotope record, and a ~ 69.5 Ma radiometric age for the lower Cantwell Formation at the East Fork Toklat River, Denali National Park and Preserve, Alaska: Implications for mid-Maastrichtian high-latitude paleoenvironments and paleoclimate.
- Sewall, J.O., van de Wal, R.S.W., van der Zwan, K., van Oosterhout, C., Dijkstra, H.A., and Scotese, C.R., 2007. Climate model boundary conditions for four Cretaceous time slices. *Climate of the Past* 3, 647–657.
- Sherwood, K.W., and Craddock, C., 1979. General geology of the central Alaska Range between the Nenana River and Mount Deborah: Alaska Division of Geological & Geophysical Surveys Alaska Open-File Report 116, 24 p., scale 1:63,360.
- Shewry, P.R., 2003. Tuber storage proteins. *Annals of Botany* 91, 755–769, DOI: 10.1093/aob/mcg084.
- Sontag, L.J., 1992. Paleomagnetism of the Paleocene Teklanika Volcanics, Central Alaska Range, Alaska. [M.S. Thesis], Mississippi State University, Mississippi, 70 p.
- Spicer, R. A., 1987. Late Cretaceous floras and terrestrial environment of Northern Alaska. In: *Alaskan North Slope Geology—Pacific*

- Section, Society of Economic Paleontologists and Mineralogists 50, 497–512.
- Spicer, R.A., 2003. Changing climate and biota. In: Skelton, P.W., Spicer, R.A., Kelley, S.P., and Gilmour, I., (eds.) *The Cretaceous World*. Cambridge University Press, 360 p.
- Spicer, R.A. and Parrish, J.T., 1990a. Late Cretaceous—early Tertiary palaeoclimates of northern high latitudes: a quantitative view. *Journal of the Geological Society, London*, 147, 329–341.
- Spicer, R.A. and Parrish, J.T., 1990b. Latest Cretaceous woods of the central North Slope, Alaska. *United States Geological Survey Circular 998*, 225–242.
- Spicer, R.A., and Herman, A.B., 2010. The Late Cretaceous environment of the Arctic: a quantitative reassessment based on plant fossils. In: Fiorillo, A.R. and McCarthy, P.J. (eds.) *Ancient Polar Ecosystems. Palaeogeography, Palaeoclimatology, Palaeoecology* 295, 423–442, DOI: 10.1016/j.palaeo.2010.02.025.
- Spicer, R.A., Wolfe, J.A., and Nichols, D.J., 1987. Alaskan Cretaceous–Tertiary floras and Arctic origins. *Paleobiology* 13 (1), 73–83.
- Spicer, R.A., Herman, A.B., and Kennedy, E.M., 2005. The sensitivity of CLAMP to taphonomic loss of foliar physiognomic characters. *Palaios* 20, 429–438.
- Stanley, R.G., 1987. Thermal maturity and petroleum source potential of the Cantwell Formation (Paleocene), Alaska Range. In: Hamilton, T.D. and Galloway, J.P., (eds.) *Geologic studies in Alaska by the United States Geological Survey during 1986*. United States Geological Survey Circular 998, 104–107.
- Stone, D. B., 1981. Triassic paleomagnetic data and paleolatitudes for Wrangellia, Alaska. *Geological Report Alaska Division Geological and Geophysical Survey* 73, 55–62.
- Stone, D.B., Panuska, B.C., and Packer, D.R., 1982. Paleolatitude versus time for southern Alaska. *Journal of Geophysical Research* 87, B5, 3697–3707.
- Sweet, A.R., Ricketts B.D., Cameron A.R., Norris D.K., 1989. An integrated analysis of the Brackett Coal Basin, Northwest Territories. *Geological Survey of Canada Paper* 89-1G, 85–99.
- Talling, P.J., Lawton, T.F., Burbanks, D.W., and Hobbs, R.S., 1995. Evolution of latest Cretaceous–Eocene non-marine deposystems in the Axhandle piggyback basin of central Utah: *Geological Society of America Bulletin* 107 (3), 297–315.
- Till, A.B., Harris, A.G., Wardlaw, B.R., and Mullen, M., 2007a. Upper Triassic continental strata of the central Alaska Range: Implications for paleogeographic reconstruction. In: Ridgway, K.D., Trop, J.M., Glen, J.M.G., and O’Neill, J.M., (eds.) *Tectonic Growth of a Collisional Continental Margin: Crustal Evolution of Southern Alaska*. Geological Society of America Special Paper 431, 191–205, DOI: 10.1130/2007.2431(08).
- Till, A.B., Roeske, S.M., Bradley, D.C., Friedman, R., and Layer, P.W., 2007b. Early Tertiary ransension-related deformation and magmatism long the Tintina fault system. Alaska. In: Till, A.B., Roeske, S.M., Foster, D.A., and Sample, J. (eds.) *Exhumation and Continental Strike-Slip Fault Systems*. Geological Society of America Special Paper 434, 233–264, DOI: 10.1130/2007.2434(11).
- Tomsich, C.S., McCarthy, P.J., Fowell, S.J. and Sunderlin, D., 2010. Paleofloristic and paleoenvironmental information from a Late Cretaceous (Maastrichtian) flora of the lower Cantwell Formation near Sable Mountain, Denali National Park, Alaska. *Palaeogeography. Palaeoclimatology. Palaeoecology* 295 (3), 389–408, DOI: 10.1016/j.palaeo.2010.02.023.
- Tomsich, C.S., McCarthy, P.J. and Fiorillo, A.R., in preparation. The depositional system and environments of the Late Cretaceous (Campanian–Maastrichtian) lower Cantwell Formation at Sable Mountain, Denali National Park and Preserve, Alaska.
- Trop, J.M. and Ridgway, K.D., 1997. Petrofacies and provenance of a Late Cretaceous suture zone thrust-top basin, Cantwell basin, central Alaska Range: *Journal of Sedimentary Research* 67 (3), 469–485.
- Trop, J.M. and Ridgway, K.D., 2007. Mesozoic and Cenozoic tectonic growth of southern Alaska: A sedimentary basin perspective. In: Ridgway,

- K.D., Trop, J.M., Glen, J.M.G., and O'Neill, J.M., (eds.) *Tectonic Growth of a Collisional Continental Margin: Crustal Evolution of Southern Alaska*. Geological Society of America Special Paper 431, 55–94, DOI: 10.1130/2007.2431(04).
- Upchurch, G., R., Otto-Bliesner, B.L., and Scotese, C., 1998. Vegetation–atmosphere interactions and their role in global warming during latest Cretaceous. *Philosophical Transactions of the Royal Society of London B* 353, 97–112.
- Van Itterbeeck, J., Bolotsky, Y., Bultynck, P., and Godefroit, P., 2005. Stratigraphy, sedimentology and palaeoecology of the dinosaur-bearing Kundur section (Zeya-Bureya Basin, Amur Region, Far Eastern Russia). *Geological Magazine* 142 (6), 735–750.
- Walker, J.D., Geissman, J.W., Bowring, S.A., and Babcock, L.E., 2013. The Geological Society of America Geologic Time Scale. *Geological Society of America Bulletin* 125 (3/4), 259–272, DOI: 10.1130/B30712.1.
- Wells, S.G. and Harvey, A.M., 1987. Sedimentologic and geomorphic variations in storm-generated alluvial fans, Howgill Fells, northwest England. *Geological Society of America Bulletin* 98, 182–198.
- Wilson, F.H., Dover, J.H., Bradley, D.C., Weber, F.R., Bundtzen, T.K., and Haeussler, P.J., 1998. Geologic map of central (Interior) Alaska. United States Geological Survey Open File Report 98-133, 2 sheets, scale 1:250,000.
- Wolfe, J.A., 1979. Temperature parameters of humid to mesic forests of Eastern Asia and relation to forests of other regions of the Northern Hemisphere and Australia. *United States Geological Survey Professional Paper* 1106, 1–37.
- Wolfe, J.A., 1987. Late Cretaceous–Cenozoic history of deciduousness and the terminal Cretaceous event. *Paleobiology* 13 (2), 215–226.
- Wolfe, J.A. and Wahrhaftig, C., 1970. The Cantwell Formation of the central Alaska Range. In: Cohee, G.V., Bates, R.G., and Wright, W.B., (eds.) *Changes in stratigraphic nomenclature by the United States Geological Survey in 1968*. United States Geological Survey Bulletin 1294-A, 41–46.
- Wolfe, J.A. and Spicer, R.A., 1999. Fossil leaf character states: multivariate analyses. In: Jones, T.P. and Rowe, N.P., (eds.) *Fossil Plants and Spores: Modern Techniques*. Geological Society, London, 233–239.
- Wright, J.L. and Breithaupt, B.H., 2002. Walking in Their Footsteps and What They Left Us: Dinosaur Tracks and Traces. In: Scotchmoor, J.G., Breithaupt, B.H., Springer, D.A., and Fiorillo, A.R., (eds.) *Dinosaurs—The Science Behind the Stories*. Society of Vertebrate Paleontology, American Geologic Institute, pp. 117–126.
- Zahid, K.M. and Barbeau, D.L., Jr., 2012. Constructing sandstone provenance and classification ternary diagrams using an electronic spreadsheet. *Journal of Sedimentary Research* 82, 131–132, DOI: 10.2110/jsr.2012.12.
- Zakharov, Y.D., Boriskina, N.G., Ignatyev, A.V., Tanabe, K., Shigeta, Y., Popov, A.M., Afanasyeva, T.B., Maeda, H., 1999. Palaeotemperature curve for the Late Cretaceous of the northeastern circum-Pacific. *Cretaceous Research* 20, 685–697.
- Zakharov, Y.D., Shigeta, Y., Popov, A.M., Velivetskaya, T.A., and Afanasyeva, T.B., 2011. Cretaceous climatic oscillations in the Bering area (Alaska and Koryak Upland): isotopic and paleontological evidence. *Sedimentary Geology* 235, 122–131, DOI: 10.1016/j.sedgeo.2010.03.012.

Appendix A

Table A-1. Isotopic U–Pb ratios and ages measured with LA–ICP–MS on zircon grains for Bentonite 1. Errors were calculated at the 2-sigma level.

Bentonite 1	Isotopic Ratios									Apparent Ages (Concordant Scans)						Preferred Age		
	U (ppm)	U Th	²⁰⁷ Pb / ²³⁵ U c	2 σ (%)	²⁰⁶ Pb / ²³⁸ U	2 σ (%)	²⁰⁷ Pb / ²⁰⁶ Pb	2 σ (%)	error corr.	²⁰⁷ Pb / ²³⁵ U	2 σ (Ma)	²⁰⁶ Pb / ²³⁸ U	2 σ (Ma)	²⁰⁷ Pb / ²⁰⁶ Pb	-2 σ (Ma)	+2 σ (Ma)	(Ma)	2 σ (Ma)
1322-01-1	240	2	0.08381	1.29	0.01163	0.08	0.05227	0.80	0.20	81.7	12.1	74.5	4.9	297.4	370.4	332.4	74.5	4.9
1322-01-2	212	3	2.10254	10.59	0.20254	0.86	0.07529	0.34	0.48	1149.6	34.7	1189.0	46.4	1076.2	90.7	88.1	1149.6	34.7
1322-01-3	216	2	0.08032	1.08	0.01180	0.08	0.04935	0.68	0.16	78.4	10.2	75.6	4.9	164.7	329.4	307.9	75.6	4.9
1322-01-4	573	2	0.08235	0.92	0.01142	0.06	0.05228	0.57	0.25	80.4	8.6	73.2	4.1	297.8	260.5	241.1	73.2	4.1
1322-01-5	66	2	0.55929	6.88	0.07294	0.45	0.05562	0.68	0.25	451.1	44.8	453.8	27.3	437.0	282.5	259.6	453.8	27.3
1322-01-6	339	1	0.07859	1.01	0.01066	0.06	0.05346	0.70	0.11	76.8	9.5	68.4	3.6	348.5	310.0	282.8	68.4	3.6
1322-01-7	109	3	0.08718	3.45	0.01068	0.10	0.05919	2.37	0.05	84.9	32.2	68.5	6.1	574.1	1015.0	768.7	68.5	6.1
1322-01-8	204	2	0.07975	6.29	0.01105	0.13	0.05235	4.16	0.03	77.9	59.2	70.8	8.2	300.8	601.5	1433.5	70.8	8.2
1322-01-9	102	3	0.10751	5.45	0.01247	0.28	0.06252	3.38	0.07	103.7	50.0	79.9	18.0	691.8	1383.6	980.3	79.9	18.0
1322-01-10	285	2	0.07828	1.62	0.01146	0.07	0.04953	1.05	0.08	76.5	15.3	73.5	4.7	173.1	346.2	458.5	73.5	4.7
1322-01-11	199	3	0.08097	2.18	0.01100	0.10	0.05339	1.48	0.08	79.1	20.5	70.5	6.5	345.4	690.8	572.5	70.5	6.5
1322-01-12	290	2	0.07821	1.17	0.01162	0.07	0.04884	0.75	0.09	76.5	11.0	74.4	4.5	140.0	280.0	343.7	74.4	4.5
1322-01-13	393	1	0.08083	1.11	0.01158	0.06	0.05064	0.70	0.15	78.9	10.5	74.2	4.0	224.6	338.1	306.3	74.2	4.0
1322-01-14	286	3	0.07694	1.33	0.01080	0.06	0.05167	0.89	0.16	75.3	12.6	69.3	3.9	270.7	421.2	372.8	69.3	3.9
1322-01-15	404	1	0.07251	1.04	0.01090	0.06	0.04823	0.69	0.16	71.1	9.9	69.9	3.8	110.5	221.0	322.8	69.9	3.8
1322-01-16	230	3	0.07438	1.35	0.01118	0.09	0.04826	0.87	0.21	72.8	12.7	71.7	5.7	111.9	223.7	401.0	71.7	5.7
1322-01-17	302	1	0.07206	1.48	0.01033	0.10	0.05059	1.05	0.21	70.7	14.1	66.3	6.3	222.3	444.7	446.0	66.3	6.3
1322-01-18	409	1	0.07982	1.57	0.01157	0.11	0.05003	0.96	0.28	78.0	14.8	74.2	6.9	196.6	393.2	418.3	74.2	6.9
1322-01-19	349	3	0.07361	0.98	0.01093	0.08	0.04886	0.67	0.21	72.1	9.3	70.1	5.1	141.0	282.0	305.0	70.1	5.1
1322-01-20	304	2	0.08054	1.56	0.01118	0.07	0.05224	1.03	0.10	78.7	14.6	71.7	4.7	296.0	483.1	420.3	71.7	4.7
1322-01-21	292	2	0.07505	1.75	0.01105	0.08	0.04926	1.16	0.08	73.5	16.5	70.8	4.9	160.3	320.5	510.5	70.8	4.9
1322-01-22	202	2	0.08924	1.58	0.01250	0.11	0.05179	0.98	0.09	86.8	14.7	80.1	7.0	276.3	463.5	405.5	80.1	7.0
1322-01-23	294	3	0.07758	1.99	0.01137	0.06	0.04947	1.27	0.08	75.9	18.8	72.9	3.8	170.2	340.5	551.6	72.9	3.8
1322-01-24	-	-	-	-	-	-	-	-	-	-	-	-	-	-	-	-	failed	-
1322-01-25	339	2	0.07587	1.71	0.01159	0.07	0.04746	1.08	0.06	74.3	16.1	74.3	4.5	72.3	144.5	502.7	74.3	4.5
1322-01-26	471	2	0.07649	0.93	0.01150	0.07	0.04824	0.58	0.28	74.8	8.8	73.7	4.7	110.8	221.7	270.2	73.7	4.7
1322-01-27	781	2	0.06655	1.08	0.01059	0.06	0.04558	0.72	0.24	65.4	10.3	67.9	4.1	0.0	0.0	314.4	0.0	0.0
1322-01-28	227	1	0.07826	12.69	0.01066	0.08	0.05327	8.64	0.01	76.5	119.7	68.3	5.0	340.2	680.4	2434.2	68.3	5.0
1322-01-29	142	2	0.07311	2.47	0.01077	0.10	0.04921	1.71	0.04	71.6	23.4	69.1	6.5	158.0	316.1	724.5	69.1	6.5
1322-01-30	315	3	0.22391	3.07	0.03076	0.21	0.05280	0.70	0.31	205.2	25.5	195.3	13.3	320.2	314.6	286.7	195.3	13.3
1322-01-31	257	2.4	0.07543	1.05	0.01137	0.07	0.04813	0.69	0.08	73.8	9.9	72.9	4.2	105.9	211.7	323.6	72.86	4.2
1322-01-32	281	2.8	0.07635	1.14	0.01164	0.07	0.04757	0.71	0.18	74.7	10.8	74.6	4.3	77.9	155.8	335.8	74.61	4.3
1322-01-33	506	2.1	0.22528	2.44	0.03224	0.21	0.05068	0.49	0.45	206.3	20.2	204.5	13.2	226.3	232.4	216.9	204.55	13.2
1322-01-34	483	1.5	0.08032	0.95	0.01118	0.05	0.05209	0.61	0.18	78.4	8.9	71.7	3.3	289.5	278.3	256.2	71.68	3.3
1322-01-35	30	3.4	0.51561	92.50	0.04091	7.32	0.09142	11.98	0.73	422.2	640.1	258.5	453.4	1455.3	2910.6	1811.6	422.22	640.3
1322-01-36	351	2.9	0.08142	1.33	0.01160	0.06	0.05092	0.82	0.19	79.5	12.5	74.3	3.9	237.1	393.8	351.3	74.33	3.9
1322-01-37	-	-	-	-	-	-	-	-	-	-	-	-	-	-	-	-	failed	-
1322-01-38	348	1.3	0.09067	1.87	0.01179	0.10	0.05577	1.15	0.20	88.1	17.4	75.6	6.1	443.4	492.5	426.9	75.56	6.1
1322-01-39	304	1.8	0.52812	3.06	0.06991	0.30	0.05479	0.29	0.44	430.6	20.3	435.6	18.2	403.5	118.9	114.6	435.64	18.2
1322-01-40	90	1.6	11.40454	65.85	0.47185	2.18	0.17530	0.86	0.54	2556.8	53.9	2491.7	96.0	2608.9	82.6	80.3	2556.80	53.9
1322-01-41	216	1.5	0.38818	3.79	0.04979	0.31	0.05655	0.54	0.33	333.0	27.7	313.2	19.2	473.9	216.9	203.2	313.22	19.2
1322-01-42	643	1.1	0.07498	0.95	0.01105	0.06	0.04922	0.62	0.21	73.4	9.0	70.8	4.0	158.1	308.3	281.7	70.84	4.0
1322-01-43	293	2.8	0.07068	1.11	0.01043	0.11	0.04917	0.88	0.09	69.3	10.5	66.9	7.2	156.1	312.1	395.2	66.86	7.2
1322-01-44	254	1.7	0.06859	1.21	0.01159	0.07	0.04292	0.77	0.07	67.4	11.5	74.3	4.4	0.0	0.0	75.7	0.00	0.0
1322-01-45	221	1.6	0.07718	1.86	0.01143	0.09	0.04899	1.22	0.04	75.5	17.5	73.2	5.7	147.1	294.2	535.9	73.25	5.7
1322-01-46	155	2.4	0.07586	1.96	0.01112	0.07	0.04947	1.29	0.07	74.2	18.5	71.3	4.7	170.4	340.8	558.5	71.29	4.7
1322-01-47	180	2.3	0.06797	2.46	0.01130	0.09	0.04361	1.58	0.08	66.8	23.4	72.5	5.7	0.0	0.0	528.8	0.00	0.0
1322-01-48	434	0.9	0.25637	2.42	0.03591	0.16	0.05178	0.46	0.35	231.7	19.5	227.4	9.8	275.7	208.9	196.3	227.43	9.8
1322-01-49	166	2.0	0.07784	2.68	0.01149	0.12	0.04914	1.73	0.05	76.1	25.2	73.6	7.3	154.4	308.8	736.3	73.64	7.3
1322-01-50	1145	3.9	0.95201	5.14	0.10778	0.44	0.06406	0.29	0.54	679.1	26.7	659.8	25.7	743.7	97.7	94.8	659.83	25.7
1322-01-51	323	1.4	0.07314	1.22	0.01052	0.08	0.05043	0.85	0.15	71.7	11.5	67.5	4.8	214.7	418.2	370.6	67.45	4.8
1322-01-52	342	2.3	0.07805	0.99	0.01111	0.06	0.05094	0.66	0.10	76.3	9.4	71.2	3.7	238.2	314.8	287.0	71.24	3.7
1322-01-53	426	3.4	0.07216	1.21	0.01125	0.08	0.04652	0.77	0.23	70.7	11.4	72.1	5.2	24.7	49.3	373.5	72.12	5.2
1322-01-54	140	1.7	0.07845	2.03	0.01069	0.09	0.05322	1.41	0.09	76.7	19.1	68.6	6.0	338.2	662.4	549.5	68.56	6.0
1322-01-55	389	1.4	0.06780	1.79	0.01016	0.08	0.04839	1.29	0.09	66.6	17.0	65.2	5.2	118.4	236.8	575.6	65.17	5.2
1322-01-56	-	-	-	-	-	-	-	-	-	-	-	-	-	-	-	-	failed	-
1322-01-57	290	2.6	0.07397	1.48	0.01055	0.11	0.05084	1.10	0.07	72.5	14.0	67.7	6.7	233.7	467.3	463.0	67.67	6.7
1322-01-58	556	5.1	0.26656	2.09	0.03740	0.14	0.05169	0.38	0.36	239.9	16.7	236.7	8.6	271.5	173.1	164.4	236.72	8.6
1322-01-59	307	1.9	0.06852	1.04	0.01007	0.06	0.04937	0.76	0.11	67.3	9.8	64.6	3.6	165.5	330.9	339.7	64.57	3.6
1322-01-60	258	2.3	0.06511	1.92	0.01012	0.08	0.04664	1.38	0.13	64.1	18.3	64.9	5.3	31.0	62.1	640.1	64.94	5.3

Table A-2. Isotopic U–Pb ratios and ages measured with LA–ICP–MS on zircon grains for Bentonite 2. Errors were calculated at the 2-sigma level.

Bentonite 2	Isotopic Ratios						Apparent Ages (Concordant Scans)						Preferred Age					
	U (ppm)	U/Th	²⁰⁷ Pb/ ²³⁵ U c	2 σ (%)	²⁰⁶ Pb/ ²³⁸ U	2 σ (%)	²⁰⁷ Pb/ ²⁰⁶ Pb	2 σ (%)	error corr.	²⁰⁷ Pb/ ²³⁵ U	2 σ (Ma)	²⁰⁶ Pb/ ²³⁸ U	2 σ (Ma)	²⁰⁷ Pb/ ²⁰⁶ Pb	-2 σ (Ma)	+2 σ (Ma)	(Ma)	2 σ (Ma)
1322-02-1	290	2.2	0.07402	1.29	0.01064	0.08	0.05044	0.89	0.14	72.5	12.2	68.3	4.8	215.1	430.2	386.7	68.3	4.8
1322-02-2	1572	1.1	0.12159	0.93	0.01771	0.09	0.04979	0.33	0.50	116.5	8.4	113.2	5.6	185.4	157.5	150.3	113.2	5.6
1322-02-3	355	1.8	0.17388	1.80	0.02579	0.13	0.04891	0.52	0.16	162.8	15.5	164.1	8.1	143.4	257.1	238.4	164.1	8.1
1322-02-4	475	1.8	0.17515	1.47	0.02507	0.10	0.05067	0.42	0.22	163.9	12.7	159.6	6.4	225.8	196.6	185.4	159.6	6.4
1322-02-5	127	1.5	0.23304	2.87	0.03117	0.16	0.05422	0.67	0.18	212.7	23.6	197.9	10.1	380.1	289.1	265.3	197.9	10.1
1322-02-6	533	3.5	0.07291	1.47	0.01118	0.05	0.04731	0.95	0.11	71.5	13.9	71.6	3.1	64.9	129.9	445.8	71.6	3.1
1322-02-7	318	2.4	0.07416	1.61	0.01111	0.11	0.04841	1.06	0.20	72.6	15.2	71.2	6.9	119.1	238.3	477.9	71.2	6.9
1322-02-8	756	3.0	0.07590	0.76	0.01146	0.04	0.04803	0.48	0.17	74.3	7.2	73.5	2.8	100.6	201.2	228.4	73.5	2.8
1322-02-9	280	2.2	0.07922	1.63	0.01140	0.10	0.05042	1.08	0.09	77.4	15.3	73.0	6.3	214.6	429.2	462.6	73.0	6.3
1322-02-10	-	-	-	-	-	-	-	-	-	-	-	-	-	-	-	-	failed	-
1322-02-11	216	3.9	0.07660	1.74	0.01165	0.09	0.04771	1.11	0.09	74.9	16.5	74.6	5.7	84.7	169.4	509.5	74.6	5.7
1322-02-12	1598	2.3	0.07916	0.68	0.01123	0.04	0.05112	0.43	0.21	77.4	6.4	72.0	2.3	246.3	198.4	187.0	72.0	2.3
1322-02-13	237	2.7	0.22422	2.16	0.03285	0.12	0.04950	0.47	0.21	205.4	17.9	208.4	7.7	171.5	227.8	212.9	208.4	7.7
1322-02-14	258	2.9	0.08917	1.40	0.01216	0.06	0.05319	0.84	0.13	86.7	13.0	77.9	4.0	336.9	378.2	338.6	77.9	4.0
1322-02-15	1086	0.9	0.07402	0.81	0.01107	0.06	0.04850	0.52	0.26	72.5	7.7	71.0	3.9	123.8	247.5	244.8	71.0	3.9
1322-02-16	3476	1.0	0.07761	0.49	0.01136	0.04	0.04955	0.29	0.38	75.9	4.6	72.8	2.7	173.8	139.7	134.0	72.8	2.7
1322-02-17	734	3.3	0.21391	1.62	0.03084	0.12	0.05031	0.38	0.22	196.8	13.6	195.8	7.7	209.2	179.4	170.1	195.8	7.7
1322-02-18	236	2.2	0.22763	2.12	0.03201	0.15	0.05158	0.48	0.23	208.2	17.5	203.1	9.3	266.8	220.0	206.1	203.1	9.3
1322-02-19	135	2.0	0.30527	3.63	0.04047	0.22	0.05471	0.62	0.33	270.5	28.3	255.7	13.5	400.4	263.4	243.5	255.7	13.5
1322-02-20	571	2.1	0.06969	0.75	0.01056	0.07	0.04785	0.52	0.29	68.4	7.1	67.7	4.4	92.1	184.2	245.8	67.7	4.4
1322-02-21	293	1.0	0.79861	4.91	0.09620	0.37	0.06021	0.34	0.42	596.0	27.7	592.1	21.7	611.1	122.9	118.4	592.1	21.7
1322-02-22	295	1.9	0.20363	2.22	0.02807	0.11	0.05261	0.58	0.14	188.2	18.7	178.5	7.1	312.1	258.8	239.6	178.5	7.1
1322-02-23	240	1.7	0.21580	1.85	0.03217	0.15	0.04866	0.42	0.23	198.4	15.4	204.1	9.1	131.3	207.4	195.1	204.1	9.1
1322-02-24	101	1.6	11.87201	58.76	0.48931	1.84	0.17597	0.71	0.58	2594.4	46.4	2567.7	79.9	2615.3	68.1	66.5	2594.4	46.4
1322-02-25	354	1.9	0.19936	2.49	0.02828	0.12	0.05112	0.63	0.18	184.6	21.1	179.8	7.7	246.3	298.2	273.2	179.8	7.7
1322-02-26	112	4.0	9.18545	78.58	0.37680	3.11	0.17680	1.11	0.71	2356.7	78.4	2061.3	145.8	2623.1	106.3	102.5	2356.7	78.4
1322-02-27	173	1.2	0.17474	2.80	0.02446	0.13	0.05181	0.84	0.12	163.5	24.2	155.8	8.3	277.0	393.0	350.5	155.8	8.3
1322-02-28	367	2.9	0.39523	5.19	0.05327	0.25	0.05381	0.70	0.21	338.2	37.8	334.5	15.6	363.3	305.6	279.1	334.5	15.6
1322-02-29	266	2.0	0.79823	5.27	0.09840	0.36	0.05883	0.37	0.30	595.8	29.8	605.0	21.2	561.0	141.5	135.5	605.0	21.2
1322-02-30	954	3.1	0.07452	0.72	0.01081	0.04	0.04999	0.48	0.17	73.0	6.8	69.3	2.6	194.4	232.6	217.1	69.3	2.6
1322-02-31	168	1.3	6.05904	31.23	0.35926	1.39	0.12232	0.52	0.58	1984.4	45.4	1978.7	66.2	1990.3	76.3	74.4	1984.4	44.9
1322-02-32	-	-	-	-	-	-	-	-	-	-	-	-	-	-	-	-	failed	-
1322-02-33	406	3.7	0.07182	0.99	0.01091	0.06	0.04773	0.66	0.12	70.4	9.4	70.0	3.7	85.7	171.5	314.5	70.0	3.7
1322-02-34	645	0.8	0.14528	1.30	0.02076	0.13	0.05076	0.44	0.38	137.7	11.6	132.4	8.3	230.0	204.5	192.4	132.4	8.3
1322-02-35	1666	3.3	0.05819	0.54	0.00851	0.05	0.04957	0.48	0.22	57.4	5.2	54.7	3.2	174.7	232.2	216.8	54.7	3.2
1322-02-36	157	2.3	0.07692	1.85	0.01075	0.09	0.05188	1.26	0.13	75.2	17.5	69.0	5.7	280.1	560.1	512.8	69.0	5.7
1322-02-37	657	1.9	0.07296	0.94	0.01060	0.05	0.04993	0.65	0.10	71.5	8.9	68.0	3.4	191.8	318.3	290.0	68.0	3.4
1322-02-38	470	2.4	0.08261	1.32	0.01126	0.08	0.05323	0.88	0.09	80.6	12.4	72.2	4.8	338.6	399.4	355.4	72.2	4.8
1322-02-39	303	2.7	0.07792	1.45	0.01054	0.08	0.05360	1.01	0.14	76.2	13.7	67.6	4.9	354.1	457.0	400.3	67.6	4.9
1322-02-40	601	3.3	0.11193	1.14	0.01557	0.07	0.05215	0.53	0.16	107.7	10.5	99.6	4.1	291.9	240.9	224.2	99.6	4.1
1322-02-41	296	1.9	0.22398	2.21	0.03091	0.13	0.05255	0.51	0.19	205.2	18.4	196.3	7.9	309.5	229.6	214.4	196.3	7.9
1322-02-42	693	3.0	0.06833	1.14	0.01076	0.05	0.04606	0.76	0.17	67.1	10.9	69.0	2.9	0.9	1.7	373.9	69.0	2.9
1322-02-43	293	2.0	0.07633	1.39	0.01080	0.07	0.05126	0.94	0.14	74.7	13.2	69.3	4.5	252.4	451.7	396.6	69.3	4.5
1322-02-44	746	2.6	0.06625	0.92	0.00949	0.05	0.05065	0.70	0.20	65.1	8.8	60.9	3.3	225.0	335.1	303.8	60.9	3.3
1322-02-45	919	1.7	0.07684	1.22	0.01053	0.08	0.05292	0.81	0.30	75.2	11.5	67.5	5.1	325.4	366.8	329.4	67.5	5.1
1322-02-46	111	2.6	0.15590	8.34	0.01048	0.29	0.10790	6.21	0.11	147.1	74.7	67.2	18.7	1764.2	1294.8	900.2	67.2	18.7
1322-02-47	288	1.5	0.11735	5.49	0.01276	0.25	0.06669	3.22	0.13	112.7	50.5	81.8	16.1	828.0	1211.8	872.3	81.8	16.1
1322-02-48	121	5.3	1.62781	12.14	0.17132	0.66	0.06891	0.49	0.30	981.0	47.5	1019.4	36.6	896.1	150.7	143.8	1019.4	36.5
1322-02-49	294	2.9	0.08024	1.43	0.01151	0.07	0.05055	0.92	0.09	78.4	13.4	73.8	4.6	220.3	440.6	395.2	73.8	4.6
1322-02-50	416	3.7	0.57981	3.64	0.07216	0.29	0.05828	0.36	0.27	464.3	23.5	449.2	17.2	540.2	137.1	131.5	449.2	17.2
1322-02-51	-	-	-	-	-	-	-	-	-	-	-	-	-	-	-	-	failed	-
1322-02-52	153	1.2	0.04873	2.20	0.00501	0.08	0.07056	3.31	0.07	48.3	21.4	32.2	5.3	944.8	1146.3	836.4	32.2	5.3
1322-02-53	654	4.3	0.25962	2.32	0.02495	0.13	0.07548	0.62	0.40	234.4	18.8	158.8	8.1	1081.3	169.7	160.9	158.8	8.1
1322-02-54	106	0.6	5.50767	28.81	0.33901	1.25	0.11783	0.56	0.43	1901.8	45.5	1881.9	60.4	1923.6	85.7	83.3	1901.8	45.0
1322-02-55	656	2.2	0.41316	2.48	0.05460	0.22	0.05488	0.31	0.37	351.1	17.9	342.7	13.4	407.2	127.7	122.8	342.7	13.4
1322-02-56	557	1.9	0.18717	1.26	0.02788	0.12	0.04870	0.31	0.34	174.2	10.8	177.2	7.5	133.2	153.6	146.8	177.2	7.5
1322-02-57	-	-	-	-	-	-	-	-	-	-	-	-	-	-	-	-	failed	-
1322-02-58	-	-	-	-	-	-	-	-	-	-	-	-	-	-	-	-	failed	-
1322-02-59	376	2.9	0.18237	1.98	0.02649	0.12	0.04993	0.53	0.23	170.1	17.1	168.6	7.8	191.6	257.1	238.3	168.6	7.8
1322-02-60	1205	1.4	0.07681	0.65	0.01110	0.05	0.05020	0.44	0.12	75.1	6.2	71.1	3.2	204.4	211.9	199.0	71.1	3.2